NACA

RESEARCH MEMORANDUM

A COMPARISON OF THE EXPERIMENTAL AND THEORETICAL LOADING OVER TRIANGULAR WINGS AT SUPERSONIC SPEEDS

By John W. Boyd and E. Ray Phelps

Ames Aeronautical Laboratory
Moffett Field, Calif.

NATIONAL ADVISORY COMMITTEE
FOR AERONAUTICS

WASHINGTON
January 3, 1951

Classification cancelled (or changed to) Unclassified

By Authority of NASA Tech Pub Announcement #207
(OFFICER OR DOD DIRECTIVE AUTHORIZING CHANGE)

By 9 Oct 56

NK
(GRADE OF OFFICER MAKING CHANGE)

4 April
DATE

NATIONAL ADVISORY COMMITTEE FOR AERONAUTICS

RESEARCH MEMORANDUM

A COMPARISON OF THE EXPERIMENTAL AND THEORETICAL LOADING OVER TRIANGULAR WINGS AT SUPERSONIC SPEEDS

By John W. Boyd and E. Ray Phelps

SUMMARY

The results of an experimental investigation of the pressure distribution over two triangular wings at supersonic speeds are presented. The two wings which were tested had identical plan forms, 45° sweepback of the leading edge, and an aspect ratio of 4.0, but different airfoil sections. One model was composed of round leading-edge sections and the other of sharp-nose, biconvex sections, 6 percent thick in streamwise planes. The experimental pressure distributions were obtained at Mach numbers from 1.20 to 1.70 at a Reynolds number of 1.8×10^6 and angles of attack from 0° to 20°.

The results showed a significant effect of leading-edge profile on the flow characteristics at high lift coefficients. For the round-nose airfoil in the lower speed range wherein the Mach lines were swept ahead of the leading edge, transonic flow characteristics were manifest in the form of a shock wave normal to the airfoil surface. Additional transonic effects were noted for the sharp-nose airfoil. A shock wave oblique to the airfoil surface was formed near the sharp leading edge and the nature of the flow was such that a somewhat higher loading was realized than that for the round-nose airfoil.

In the higher speed range wherein the Mach lines were swept behind the leading edge, flow characteristics similar to those experienced at the lower Mach numbers were evident, since, as a result of the detached bow wave, flow interaction occurred between the lower and upper surface.

Despite the existence of these transonic flow phenomena, the agreement between the load distribution given by the linear supersonic theory and by experiment was reasonably good.

INTRODUCTION

The validity of the linear theory in predicting the load distribution over triangular wings at supersonic speeds has been the subject of a number of experimental investigations. The theoretical methods, of necessity, involve certain simplifying assumptions which limit their application to cases where viscosity and higher-order effects are negligible.

Experimental investigations to date have shown the experimental load distributions to be in good agreement with the theoretical at low angles of attack. At high angles of attack, however, where the basic assumptions of the theory are not applicable, the experimental load distributions show a marked deviation from theory. Mr. Clinton Brown of the Langley Laboratory has pointed out that there is a correlation between the experimental data obtained for triangular wings at high lift coefficients at supersonic speeds and data presented in reference 1 for two-dimensional airfoils at transonic speeds. An experiment was undertaken for the purpose of pursuing this correlation further. Data were also obtained to determine the effect of leading-edge profile and to provide results for a comparison between the theoretical and experimental load distributions.

SYMBOLS

$\frac{b}{2}$ semispan, feet

c local wing chord, feet

c_r root chord, feet

$\bar{c}$ mean aerodynamic chord measured parallel to the plane of symmetry

$$\left(\frac{\int_0^{b/2} c^2 dy}{\int_0^{b/2} c\, dy} \right), \text{ feet}$$

C_N normal-force coefficient

M free-stream Mach number

P pressure coefficient $\left(\frac{p-p_o}{q_o}\right)$

P_{vac} value of pressure coefficient P corresponding to a complete vacuum on the upper surface of the airfoil

$\frac{\Delta p}{q_o \alpha}$ loading coefficient per unit angle of attack $\left(\frac{p_l-p_u}{q_o \alpha}\right)$, per degree

p local pressure on airfoil, pounds per square foot

p_o free-stream static pressure, pounds per square foot

q_o free-stream dynamic pressure $\left(\frac{1}{2}\rho V^2\right)$, pounds per square foot

R Reynolds number based on mean aerodynamic chord

V velocity of free stream, feet per second

$\frac{w}{2}$ half-width of plan form at any point, feet

$\frac{x}{c_r}$ chordwise station, fraction of root chord measured parallel to plane of symmetry

$\frac{y}{w/2}$ spanwise station, fraction of local half-width of plan form

α angle of attack of wing at plane of symmetry, degrees

β $\sqrt{M^2-1}$

ϵ vertex half-angle of wing plan form, degrees

μ Mach angle $\left(\sin^{-1} 1/M\right)$, degrees

ρ mass density of free stream, slugs per cubic foot

Subscripts

l conditions on lower surface of airfoil

u conditions on upper surface of airfoil

[redacted]

APPARATUS AND MODELS

The experimental investigation was conducted in the Ames 6- by 6-foot supersonic wind tunnel which is a closed-return variable-pressure type with a Mach number range of 1.15 to 2.0. This wind tunnel is described fully in reference 2.

A sketch of the 45° swept-back triangular-wing models which gives all plan-form dimensions is shown in figure 1. In order to obtain as high a test Reynolds number as possible, the maximum size model which was free from wind-tunnel-wall interference at the lowest test Mach number was used.

Since reference 1 had shown a pronounced effect of airfoil-thickness distribution on the flow characteristics of airfoil sections at transonic speed and, since in the present experiment it was expected that similar transonic effects would be manifest, two different airfoil sections were selected for the wings. One wing was composed of round-nose airfoil sections, 6 percent thick in streamwise planes. The section used for this wing was the NACA 0006-63 profile. The other wing was composed of sharp-nose, biconvex sections, 6 percent thick in streamwise planes with the maximum thickness at 30 percent of the chord. (See reference 1.) See table I for airfoil ordinates.

The models were cast of bismuth-tin alloy and coated with zinc chromate to give a smooth surface. The cone which joined the wing to the support sting (fig. 2) was designed to minimize the pressure disturbance over the wing and, at the same time, fulfill the strength requirements. The support sting itself served as a conduit for the pressure tubes.

The right wing panel was fitted with 86 pressure orifices, each 0.013 inch in diameter, arranged to measure both the local pressure on the surface and the pressure difference between the upper and the lower surfaces. These orifices were located in planes perpendicular to the plane of symmetry at three chordwise stations (fig. 1). These stations, hereafter designated as stations 1, 2, and 3, were located at 25, 50, and 75 percent of the root chord, respectively.

The models were mounted vertically in the test section on the end of a cantilever sting support as shown in figure 2. The sting angle of attack could be adjusted to any angle between ±17.5° while the tunnel was operating. Since it was desired to obtain angles of attack up to a maximum of 20°, a 5° bent sting was used which gave an angle range of −12.5° to 22.5°. The model angle of attack during the test was influenced by the deflection of the model support under load. An arrangement of mirrors and lenses was used to determine optically the true angle of attack.

METHODS

Theoretical

In reference 3 it is shown that, by a suitable distribution of line sources and sinks having a common point of intersection, it is possible to obtain solutions for the pressure distribution over the surface of triangular wings at zero lift. Since the method is limited in application to thin airfoils with sharp leading edges, a quantitative comparison between the theoretical computations and the experimental results would be more significant for the case of the sharp-nose wing.

The theoretical loading per unit angle of attack was calculated using the method of references 4, 5, and 6. The flow field of a lifting triangular wing is of conical form; that is, quantities such as pressure and velocity are constant along rays emanating from the apex of the wing. The flow, therefore, when shown in transverse planes has a characteristic of two-dimensional flow in that the pressure plots at all fore and aft locations will be similar.

Since the theory is based on linear differential equations, the principle of superposition applies so that the pressure distribution due to airfoil thickness has no influence on the pressure distribution due to angle of attack, or vice versa.

Experimental

Tests.- A major portion of the data was obtained over a Mach number range of 1.20 to 1.70 at a constant Reynolds number of 1.8 million and at angles of attack from 0° to 20°. A limited amount of data was obtained at Reynolds numbers of 1 million and 3.75 million. For a Mach number of 1.20 and 20° angle of attack, reliable data were not obtained since, at these conditions, the data indicated that the flow in the test section was choked.

Recording and reduction of data.- The pressures were indicated on multiple-tube manometers which were photographed to record the pressures. The data were reduced directly to spanwise plots of the pressure coefficient through use of a pressure plotting machine.

Precision.- Surveys of the wind-tunnel air stream (reference 3) have shown that, at Mach numbers other than M = 1.4, there exist significant pressure and stream-angle disturbances in the air stream. These

surveys indicate, however, that the flow in the air stream is two-dimensional; that is, there are no appreciable transverse pressure gradients in horizontal planes. In the present test, therefore, the model was mounted vertically to minimize the effects of stream irregularities on the load distribution. Since the flow was similar in all vertical planes, the static pressure results obtained in the vertical plane at the center line of the tunnel (reference 3) were used to correct the measured pressures for all test conditions. In applying these corrections, it was assumed that the static pressures on the upper and lower surfaces were equally affected by the stream static pressure variation and that the lifting pressures were not affected. These assumptions were shown to be valid by the results of the investigation of reference 3.

The major items which may cause inaccuracies in the experimental pressure distributions have been noted in reference 7. Since the techniques employed in this investigation parallel those used in reference 7, the over-all precision should be of the same magnitude; that is the wing static pressures should be accurate to within ±1 percent of the test dynamic pressures.

As was noted previously, the size of the wing was chosen so that even at the low Mach numbers there was no interference between the wing and the compression or expansion waves originating on the model and reflecting from the tunnel walls.

Errors made in measuring the angle of attack were confined to purely mechanical inaccuracies since the variation of the stream angle in the region of the model was negligible. A possible error of ±0.05° in the angle of attack was incurred in the initial referencing of the model with respect to the stream direction. The angle of attack during the test, determined by means of the optical measuring system, could be read accurately to within ±0.03°, resulting in a total possible error of ±0.08° in the angle-of-attack reading.

The absolute humidity of the air in the wind tunnel was kept below 0.0003 pound of water per pound of air at all times so that it had negligible effect on the experimental results.

RESULTS AND DISCUSSION

Pressure-distribution measurements were made on the two triangular wings for a range of Mach numbers from 1.20 to 1.70 at a constant Reynolds number of 1.8 million and at angles of attack from 0° to 20°. For the purpose of discussion in this report, figures showing pressure distributions due to airfoil thickness are presented only for Mach numbers

of 1.30, 1.53, and 1.70, and the pressure distributions due to angle of attack are presented at 1.30 and 1.70. These data are considered representative of the results obtained throughout the test range. The experimental results for the complete range of test variables are presented in table II in the form of pressure coefficients for any further analysis the reader may wish to make. A portion of the data of station 3 was omitted from this tabulation because of noticeable interference effects from the support cone.

Pressure Distribution at Zero Lift

Experimental values of the pressure distribution at approximately zero angle of attack are compared with theoretical values in figure 3 for Mach numbers of 1.30, 1.53, and 1.70. Due to the limitation of the theoretical method, a qualitative comparison between theory and experiment for the round-nose airfoil was not considered.

Examination of the experimental data for the sharp-nose airfoil at $M = 1.30$ showed the agreement between the predicted and measured pressure distributions to be good at station 1 with somewhat poorer agreement at stations 2 and 3. At these latter stations, the theoretical pressure peak, associated with the discontinuity in the radius of curvature of the airfoil surface at the point of maximum thickness, was not as pronounced in the experimental data. Although no complete explanation of this difference between theory and experiment has been definitely established, much of the difference may be attributed to boundary layer and second-order compressibility effects.

At Mach numbers of 1.53 and 1.70, the agreement between theory and experiment generally was not as good as at a Mach number of 1.30, the correlation being particularly poor near the airfoil leading edge. The combinations of Mach number, leading-edge sweep, and airfoil wedge angle were such that the leading-edge shock wave was detached for all angles of attack. The theory for Mach lines swept behind the leading edge (in this case for $M = 1.53$ and 1.70) assumes an attached wave and cannot account properly for the mixed subsonic and supersonic flow that existed between the detached bow wave and the leading-edge of the airfoil. For these Mach numbers, the deviation between theory and experiment may be attributed, therefore, to the detached shock.

Flow Characteristics and Pressure Distribution at Angles of Attack

In the analysis of the experimental lifting pressures, it was found that, even though theory and experiment did not always agree on the magnitude of the pressures on the wing, the experimental lifting pressures were, as predicted by theory, essentially constant along rays from the apex of the wing. It is possible, therefore, and convenient in considering the flow over triangular wings to resort to transverse pressure plots, since they are essentially similar at all fore- and aft-locations, because for both theory and experiment the pressures tend to be constant along rays. Components of velocity perpendicular to rays are considered in analyzing these transverse pressure plots. It may be seen that on the surface of wings moving at supersonic speeds the components may be either subsonic or supersonic, depending on the stream Mach number and the sweep of the ray considered.

It has been shown previously that, in discussing the flow over triangular wings, it is convenient to define the supersonic speed ranges by the variable $\tan \epsilon / \tan \mu$ where ϵ is the semivertex angle of the wing and μ is the Mach angle. Values of $\tan \epsilon / \tan \mu$ greater than 1.0 correspond to a supersonic leading edge and values less than 1.0 correspond to a subsonic leading edge. A value of $\tan \epsilon / \tan \mu$ of 1 corresponds to sonic velocity perpendicular to the wing leading edge.

Mach lines swept ahead of the leading edge.- Experimental pressure distributions for both the round-nose and sharp-nose airfoil for station 2 are presented in figure 4 for several angles of attack and for a Mach number of 1.30. The data presented here are typical of the results obtained in this speed range (Mach lines swept ahead of the leading edge). Examination of these data shows the existence of certain pressure discontinuities, usually associated with shock waves, which are not revealed by the theoretical analysis. For the sharp-nose airfoil at an angle of attack of 5°, the data show a pressure peak near the airfoil leading edge, followed immediately by an abrupt compression. At 10° angle of attack, the negative pressure peak was followed by a region of less negative pressures which was, in turn, followed by a compression at about 70 percent of the semispan. It should be noted that at 10° angle of attack, the pressure coefficient near the leading edge approached the absolute physical limit. The magnitude of this limit P_{vac} is indicated in the figure. At 15° and 20° angles of attack, therefore, since nearly an absolute vacuum had already been attained on the upper surface at the lower angles of attack, only a slight increase in the magnitude of the upper-surface pressure coefficients near the leading edge was possible. Further, the low-pressure region, which was localized into a pressure peak near the leading edge at the low angles of attack, spread over a

wide region of the airfoil surface at these high angles of attack. The data indicated that the wide region of negative pressure coefficients (very nearly equal to a full vacuum) was terminated by a compression at about 40 percent of the semispan.

For the round-nose airfoil, no abrupt compression in the pressures was noted at an angle of attack of 5°. At an angle of attack of 10°, however, a region of large negative pressure coefficients was noted which was terminated by a compression at about 50 percent of the semispan. The data for 15° and 20° angles of attack showed a wide region of negative pressure coefficients very nearly equal to a full vacuum. This region of large negative pressure coefficients was terminated by a compression between 50 and 60 percent of the semispan.

A study of the pressure data just discussed reveals certain pressure discontinuities over the airfoil surface which are similar to those noted in the data obtained from two-dimensional airfoils with corresponding profiles at transonic speeds (reference 1). It has been shown in reference 1 that the pressure discontinuities noted on the surface of the two-dimensional airfoil at transonic speeds were a result of shock waves. Due to the similarity in the pressure data, it was concluded that the pressure discontinuities noted in the data of the present investigation also denoted the existence of shock waves and that consequently the shock patterns in transverse sections would resemble closely the patterns existing on the two-dimensional airfoils at transonic speeds (shown in the schlieren photograph of fig. 5). An estimate of the flow pattern, as deduced from the foregoing correlation, for triangular wings with Mach lines ahead of the leading edge ($\tan \epsilon / \tan \mu < 1.0$) is sketched in figure 6. This sketch is for a representative set of test conditions at any transverse section; the pattern will change in detail as Mach number and lift coefficient vary but its basic character should remain as sketched.

For the round-nose airfoil, due to the easy curvature of the round leading edge, a gradual expansion of the streamlines around the airfoil leading edge occurred, and the local velocity components on the upper surface perpendicular to rays from the apex were sufficiently large at high angles of attack as to result in a local region of supersonic flow which was terminated by a shock wave, as was indicated by the compression in the pressure data. The shock wave, which was normal to the airfoil surface but oblique to the supersonic stream, corresponds to the usual normal shock wave which has been noted on two-dimensional airfoils at transonic speeds (fig. 5).

For the sharp-nose airfoil additional transonic flow characteristics were deduced from the pressure data. A marked similarity can be noted in the estimated flow characteristics presented in figure 6 for the sharp-nose airfoil of the present test and the flow over a sharp two-dimensional

[redacted]

airfoil at transonic speeds as evidenced by the schlieren photograph of figure 5. For triangular wings swept behind the Mach lines, upwash occurs around the airfoil leading edge as a result of the flow interaction between the upper and lower surfaces. The air, in flowing from the lower to the upper surface, is required to turn abruptly around the sharp leading edge, resulting in a highly complex mixed subsonic and supersonic flow field. Although the present state of knowledge of what occurs in this flow field is limited, the nature of the flow is apparently analogous to the flow around a sharp convex corner which was treated by Busemann in reference 8. A cursory study of the problem has indicated that the location and curvature of the sonic line in the region near the airfoil nose were such that the streamlines above the nose turned toward the airfoil and the flow impinged on the upper surface of the airfoil. Since the streamlines must turn and flow along the airfoil surface, a distributed compression region resulted, which coalesced into a finite shock wave oblique to the airfoil surface. Behind this oblique shock wave was a region of lower supersonic velocities which was terminated by a normal shock wave. This hypothesis appears to be consistent with the observed flow patterns of figure 6 and with the experimental results of the present test. It is interesting to note that the compression which was observed for the sharp leading-edge airfoil near the nose was not evident for the round-nose airfoil. This is to be expected since the curvature of the round leading edge permits a more gradual expansion of the streamlines around the airfoil leading edge.

The experimental and theoretical load distributions for the two triangular wings are presented in figure 7. The effects of the transonic flow characteristics just discussed are apparent in the differences between the theoretical and experimental loading. The data for the round-nose airfoil at 5° angle of attack include experimental loading coefficients which are greater than those given by theory. For 10° angle of attack, also, the experimental loading was generally greater than the theoretical values over a large portion of the airfoil surface. As expected, there was a decrease in the experimental loading at the location of the normal shock wave. For 15° and 20° angles of attack, the experimental loading near the leading edge was much less than the theoretical because of the previously mentioned physical limitation on the magnitude of the upper-surface pressure coefficients which was not considered by theory. Over the remaining portion of the span, the experimental loading lay generally above the theoretical.

The experimental loading data for the sharp-nose airfoil showed that the transonic effects were also evident (see fig. 7). At an angle of attack of 5°, the influence of the sharp leading edge was manifest in a region of loading coefficients near the leading edge which were somewhat greater than those for the round-nose airfoil, followed by a spanwise variation of the loading coefficients that was in somewhat better agreement with the theoretical loading than the data for the round-nose

airfoil. For an angle of attack of 10°, the loading coefficients for the sharp-nose airfoil were not as high as those at 5° angle of attack but were somewhat greater than those for the round-nose airfoil at 10° angle of attack. The location of the shock wave normal to the airfoil surface may be discerned in the discontinuities of the spanwise load distribution. As in the case of the round-nose airfoil, at 15° and 20° angles of attack, the experimental load distribution near the leading edge fell considerably below the theoretical value.

Mach lines swept behind the leading edge.- Experimental pressure distributions for both the round-nose and the sharp-nose airfoils are presented in figure 8 for several angles of attack at a Mach number of 1.70. It is evident from a study of the pressure data that, even though the theoretical flow velocity component perpendicular to the leading edge was supersonic, the characteristics of the flow differed little from those in the lower speed range wherein the flow component perpendicular to the leading edge was subsonic. Although the pressure discontinuities were considerably softened, the shape of the pressure-distribution curves was quite similar to those in the lower speed range.

At these higher supersonic speeds, where the value of $\tan \epsilon / \tan \mu$ is greater than 1.0 but less than the value for which the shock wave became attached to the sharp leading edge, the flow pattern over both wings, as deduced from available pressure data, was as sketched in figure 9. For the round-nose airfoil, a detached bow wave occurred ahead of the swept leading edge. Since, in the region between the detached bow wave and the leading edge, the flow components perpendicular to the leading edge were subsonic, the flow around the leading edge of the airfoil was similar to the flow experienced when the Mach line was ahead of the leading edge. The local velocity components on the upper surface perpendicular to a ray from the apex were large enough to cause a local region of supersonic flow which was terminated by a normal shock wave, as in typical transonic two-dimensional flow.

For the sharp-nose airfoil, the detached bow wave was also present since the wedge angle was greater than the value for shock attachment. There existed a small region of subsonic flow components in the vicinity of the leading edge which resulted in flow interaction between the upper and lower surfaces. The flow characteristics were similar to those noted previously for Mach numbers at which the Mach lines were swept ahead of the leading edge. Transonic flow similar to that noted for the lower speed range occurred, though the extent of the influence of the sharp leading edge was not as great, since the upwash angle at the wing leading edge was not as large as at the lower Mach numbers. This reduction in the upwash angle was due to the fact that the flow interaction between the upper and lower surface was confined to the region between the detached bow wave and the leading edge.

The experimental and theoretical load distributions for the two triangular wings are presented in figure 10. The effects of the [redacted]

transonic flow characteristics just discussed are apparent in the experimental load distribution. Since $\tan \epsilon / \tan \mu$ is greater than unity, it is assumed in the theory that the bow wave is attached to the wing leading edge with the result that the lifting pressures are constant between the Mach line and the leading edge. In the actual case, however, since the bow wave was detached, flow interaction between the upper and lower surfaces occurred, resulting in a peak in the loading at the leading edge. The sharp-nose airfoil showed a somewhat higher loading peak near the leading edge than did the round-nose airfoil due to the previously discussed flow phenomena. Force data presented in reference 9 have shown that, as the Mach number for complete shock attachment to the leading edge is approached, the agreement between theory and experiment may be expected to be improved.

Reynolds number effects.- A limited amount of data was obtained for the round-nose airfoil at Reynolds numbers of 1 million and 3.75 million for an angle of attack of 5°. As shown in figure 11 for Mach numbers 1.30 and 1.70, the data indicate a negligible effect of Reynolds number variation on the spanwise load distribution for Reynolds numbers of 1.8 million to 3.75 million. At a Mach number of 1.30, however, the experimental data show the loading coefficients at a Reynolds number of 1 million to be somewhat less than the values obtained at higher Reynolds numbers. As the Mach number is increased from 1.30 to 1.70, the effect of Reynolds number becomes negligible. Since no Reynolds number effects were found in the range from 1.8 million to the maximum value attainable, 3.75 million, the major portion of this test was conducted at a Reynolds number of 1.8 million for reasons of economy.

It is noteworthy that, at the highest angle of attack ($\alpha = 20°$, approx.) at all Mach numbers investigated, most of the airfoil upper surface was subjected to pressures nearly equivalent to a full vacuum. It is believed, therefore, that the action of viscous forces will be negligible when compared with pressure forces so that Reynolds number effects at these high lifts may not be significant.

Normal-Force Coefficients

Figure 12 presents a comparison of the experimental and theoretical normal-force coefficients versus angle of attack for Mach numbers of 1.20, 1.30, 1.53, and 1.70. The experimental normal-force coefficients were obtained by a mechanical integration of the spanwise pressure plots at each of the angles of attack. Excluding the data at 15° and 20° angles of attack which fall below the theoretical curve at all Mach numbers, the normal-force coefficients exhibit a trend with Mach number similar to that discussed in reference 9. In the lower speed range ($\tan \epsilon / \tan \mu < 1.0$ ($M = 1.20$)), the sharp-nose and the round-nose

airfoils give values of the normal-force coefficient that fall somewhat above those predicted by the linear theory. As the value of $\tan \epsilon / \tan \mu$ of 1.0 is approached and slightly exceeded, the normal force first equals the predicted value at a Mach number of 1.30 and then falls slightly below the predicted value at a Mach number of 1.53. However, in the higher supersonic speed range where $\tan \epsilon / \tan \mu$ is greater than 1.0 ($M = 1.70$), the experimental normal-force coefficients agree more closely with the linear theory as a result of the approaching attachment of the bow wave to the airfoil leading edge. Previous tests have shown that as the Mach number for complete shock attachment to the leading edge was approached, good agreement between the measured and predicted loading may be expected. (See reference 9.)

As mentioned previously, at the higher angles of attack (15° and 20°) the experimental normal-force coefficients fall below the values predicted by the linear theory. This difference between theory and experiment is to be expected, of course, since the basic assumptions of the theory obviously are invalid when the pressure coefficients approach a value equivalent to a full vacuum.

Application of Results to Other Triangular Wings

The foregoing discussion has shown that significant transonic flow effects occur on triangular wings at supersonic speed and that these transonic flow characteristics show marked similarity to those which have been noted for the two-dimensional airfoil sections at high subsonic speeds. There remains the question, however, of the means by which the results presented herein for 45° triangular wings may be applied to other triangular wings of different sweepback and airfoil section. At the present time only a qualitative relation can be shown to exist.

The linear theory yields the parameters β and $\tan \epsilon / \tan \mu$ as relating the characteristics of triangular wings of different sweepback at supersonic speeds in that the load distribution, the lift-curve slope, the curvature of the drag parabola, and the moment-curve slope are given as functions of β and $\tan \epsilon / \tan \mu$. In the linear theory, however, only small velocity increments are considered, a condition which obviously is not applicable at high lift coefficients. It is clear from the foregoing discussions that the transonic effects, which were noted, are primarily a function of (a) the Mach number of the flow component perpendicular to the swept leading edge and (b) the shape of the airfoil in the vicinity of the wing leading edge. It appears, therefore, that the correlating parameter insofar as the flow characteristics at high lift coefficients are concerned should be $\sin \epsilon / \sin \mu$ which is a

measure of the Mach number perpendicular to the leading edge. It is to be expected that, for other triangular wings of similar leading-edge radius or wedge angle, flow characteristics similar to those found for the wings of the present test will be experienced for the same values of $\sin \epsilon / \sin \mu$.

With regard to the airfoil nose shape the following qualitative correlation may be stated: For wings of smaller wedge angles, the transonic flow characteristics noted will occur at lower lift coefficients. Further, round-nose airfoils of much smaller nose radii may be expected to give flow characteristics similar to airfoils with sharp leading edges.

CONCLUDING REMARKS

Pressure-distribution measurements over a sharp-nose and a round-nose airfoil of triangular plan form were made for a Mach number range of 1.20 to 1.70 to determine the effect of leading-edge profile and to provide data for a comparison of the experimental and theoretical load distribution.

The results of the tests indicated a significant effect of leading-edge profile on the flow characteristics at high lift coefficients. For the round-nose airfoil in the lower speed range where the Mach lines are swept ahead of the leading edge, transonic-flow characteristics similar to those experienced on round-nose, two-dimensional airfoils at transonic speeds were manifest in the form of a region of supersonic velocity near the airfoil leading edge which was terminated by a normal shock wave. An additional transonic effect was noted at the leading edge of the sharp-nose airfoil. A shock wave oblique to the airfoil surface was formed and the nature of the flow was such that a somewhat higher loading was realized than that for the round-nose airfoil. Despite the existence of these transonic flow phenomena, the agreement between the theoretical and experimental load distribution was reasonably good up to an angle of attack of 10°, the sharp-nose airfoil exhibiting generally better agreement. Further increase in angle of attack resulted in the experimental loading near the leading edge falling below theory because of the physical limitation of zero pressure on the magnitude of the upper-surface pressure coefficient.

In the higher speed range, where the Mach lines were swept behind the leading edge, since the leading-edge bow wave was detached with resulting flow interaction between the lower and upper surfaces, the flow characteristics were similar to those experienced in the lower speed range wherein the Mach lines were swept ahead of the leading edge. Reasonably good agreement between the measured and predicted loading was also realized in this speed range. As the speed is increased further so that the

bow wave approaches attachment to the leading edge, it is expected that the correspondence between theory and experiment would be further improved.

The experimental normal-force coefficients for both the round-nose and the sharp-nose airfoils were essentially the same and were slightly higher than the theoretical values in the low-speed range (M = 1.20). Increasing the Mach number to 1.53 caused the experimental values to fall slightly below the predicted results. Further increase in Mach number resulted in closer agreement between the theoretical and experimental normal-force coefficients since, as previously mentioned, the bow wave was approaching complete attachment to the airfoil leading edge.

Ames Aeronautical Laboratory,
National Advisory Committee for Aeronautics,
Moffett Field, Calif.

REFERENCES

1. Lindsey, W. F., Daley, Bernard N., and Humphreys, Milton D.: The Flow and Force Characteristics of Supersonic Airfoils at High Subsonic Speeds. NACA TN 1211, 1947.

2. Frick, Charles W., and Olson, Robert N.: Flow Studies in the Asymmetric Adjustable Nozzle of the Ames 6- by 6-Foot Supersonic Wind Tunnel. NACA RM A9E24, 1949.

3. Jones, Robert T.: Thin Oblique Airfoils at Supersonic Speeds. NACA TN 1107, 1946.

4. Gurevich, M. I.: Lift Force of an Arrow-Shaped Wing. Prikladnaia Matematika i Makanika (Moscow) vol. X, no. 4, 1946, pp. 513-520.

5. Stewart, H. J.: The Lift of a Delta Wing at Supersonic Speeds. Quart. App. Math., vol. IV, no. 3, Oct. 1946, pp. 246-254.

6. Brown, Clinton E.: Theoretical Lift and Drag of Thin Triangular Wings at Supersonic Speeds. NACA Rep. 839, 1946.

7. Frick, Charles W., and Boyd, John W.:. Investigation at Supersonic Speed (M = 1.53) of the Pressure Distribution Over a 63° Swept Airfoil of Biconvex Section at Zero Lift. NACA RM A8C22, 1948.

8. Busemann, Adolf: A Review of Analytical Methods for the Treatment of Flows with Detached Shocks. NACA TN 1858, 1949.

[redacted]

9. Love, Eugene S.: Investigations at Supersonic Speeds of 22 Triangular Wings Representing Two Airfoil Sections for Each of 11 Apex Angles. NACA RM L9D07, 1949.

TABLE I.- AIRFOIL ORDINATES

[Stations and Ordinates Given in Percent of Airfoil Chord]

NACA 0006-63				Sharp-Nose Biconvex Profile			
Upper surface		Lower surface		Upper surface		Lower surface	
Station	Ordinate	Station	Ordinate	Station	Ordinate	Station	Ordinate
0	0	0	0	0	0	0	0
1.25	.95	1.25	-.95	5	.92	5	-.92
2.5	1.31	2.5	-1.31	10	1.67	10	-1.67
5.0	1.78	5.0	-1.78	15	2.25	15	-2.25
7.5	2.10	7.5	-2.10	20	2.67	20	-2.67
10	2.34	10	-2.34	25	2.92	25	-2.92
15	2.67	15	-2.67	30	3.00	30	-3.00
20	2.87	20	-2.87	40	2.94	40	-2.94
25	2.97	25	-2.97	50	2.75	50	-2.75
30	3.00	30	-3.00	60	2.45	60	-2.45
40	2.90	40	-2.90	70	2.02	70	-2.02
50	2.65	50	-2.65	80	1.47	80	-1.47
60	2.28	60	-2.28	85	1.15	85	-1.15
70	1.83	70	-1.83	90	.79	90	-.79
80	1.31	80	-1.31	95	.40	95	-.40
90	.72	90	-.72	100	0	100	0
95	.40	95	-.40				
100	(.06)	100	(-.06)				
100	0	100	0				
L.E. radius: 0.40							

TABLE II.- EXPERIMENTAL PRESSURE COEFFICIENTS

(a) M = 1.20.

Station		Round-nose airfoil								Sharp-nose airfoil							
		α=0		α=5.1		α=10.4		[1]α=15.4		α=0		α=5.1		α=10.4		[1]α=15.6	
x/c_r	$\frac{y}{s/2}$	P_u	P_l	P_u	P_l	P_u	P_l	P_u	P_l	P_u	P_l	P_u	P_l	P_u	P_l	P_u	P_l
0.25	0	-0.009	0.008	-0.135	0.163	-0.228	0.359	-0.281	0.670	0.042	0.052	-0.076	0.276	-0.174	0.360	-0.238	0.666
	.267	-.008	.007	-.147	.170	-.247	.371	-.308	.684	.050	.076	-.081	.310	-.189	.400	-.238	.699
	.400	-.005	.020	-.168	.186	-.265	.390	-.313	.705	.070	.105	-.065	.320	-.191	.433	-.404	.727
	.533	.005	.028	-.175	.211	-.309	.423	-.618	.733	.108	.146	-.050	.348	-.192	.489	-.624	.770
	.667	- - -	.034	- - -	.238	- - -	.468	- - -	.776	.155	.180	-.028	.362	-.216	.544	-.703	.815
	.733	.027	.048	-.258	.269	-.552	.506	-.811	.809	.187	.217	.005	.374	-.281	.579	-.740	.849
	.800	.010	.051	-.309	.299	-.580	.543	-.792	.849	.228	.280	.007	.443	-.431	.651	-.778	.893
	.867	.052	.082	-.336	.362	-.617	.612	-.788	.892	.282	.336	.050	.551	-.618	.723	-.766	.942
	.933	.093	.240	-.294	.530	-.604	.748	-.777	.956	.374	.398	-.285	.638	-.755	.803	-.775	.974
	.100	- - -	.539	- - -	.747	- - -	.792	- - -	.739	- - -	- - -	- - -	- - -	- - -	- - -	- - -	- - -
0.50	0	-.091	-.080	-.228	.079	-.305	.378	-.341	.625	-.073	-.030	-.193	.087	-.290	.356	-.330	.610
	.133	-.097	-.076	-.237	.083	-.326	.374	-.363	.622	-.076	-.053	-.201	.083	-.307	.351	-.338	.607
	.267	- - -	-.084	- - -	.068	- - -	.354	- - -	.616	-.094	-.069	-.223	.087	-.333	.347	-.331	.612
	.400	-.120	-.095	-.270	.070	-.369	.346	-.508	.618	- - -	-.090	- - -	.079	- - -	.349	- - -	.613
	.467	-.137	-.100	-.288	.071	-.388	.351	-.592	.622	-.129	-.087	-.278	.107	-.389	.368	-.694	.624
	.533	-.136	-.116	-.306	.059	-.374	.347	-.594	.624	-.136	-.102	-.293	.084	-.406	.354	-.714	.612
	.600	- - -	-.114	- - -	.078	- - -	.354	- - -	.637	- - -	-.089	- - -	.106	- - -	.350	- - -	.629
	.667	-.142	-.120	-.353	.087	-.662	.367	-.721	.656	-.116	-.092	-.292	.102	-.453	.348	-.654	.645
	.733	-.129	-.106	-.392	.110	-.673	.389	-.721	.678	-.099	-.060	-.289	.139	-.633	.387	-.669	.679
	.800	-.121	-.088	-.441	.143	-.698	.427	-.724	.711	-.052	.007	-.263	.203	-.660	.449	-.662	.723
	.867	-.109	-.070	-.507	.200	-.738	.483	-.739	.762	.030	.082	-.208	.291	-.677	.522	-.672	.782
	.900	-.105	-.068	-.526	.225	-.766	.518	-.760	.791	.055	.131	-.182	.348	-.704	.572	-.691	.816
	.933	-.100	-.025	-.585	.298	-.786	.582	-.781	.834	.114	.213	-.335	.434	-.754	.645	-.627	.854
	.967	-.013	.055	-.447	.419	-.794	.684	-.793	.870	.192	.293	-.554	.545	-.835	.731	-.631	.893
	.100	- - -	.536	- - -	.646	- - -	.595	- - -	.432	- - -	- - -	- - -	- - -	- - -	- - -	- - -	- - -
0.75	0	- - -	- - -	- - -	- - -	- - -	- - -	- - -	- - -	- - -	- - -	- - -	- - -	- - -	- - -	- - -	- - -
	.177	- - -	- - -	- - -	- - -	- - -	- - -	- - -	- - -	- - -	- - -	- - -	- - -	- - -	- - -	- - -	- - -
	.266	- - -	- - -	- - -	- - -	- - -	- - -	- - -	- - -	- - -	- - -	- - -	- - -	- - -	- - -	- - -	- - -
	.356	- - -	- - -	- - -	- - -	- - -	- - -	- - -	- - -	- - -	- - -	- - -	- - -	- - -	- - -	- - -	- - -
	.446	- - -	-.097	- - -	.231	- - -	.394	- - -	.563	-.139	-.125	-.303	.205	-.420	.379	-.580	.545
	.533	-.162	-.132	-.331	.113	-.492	.385	-.458	.564	-.167	-.143	-.340	.140	-.450	.357	-.590	.546
	.578	-.179	-.149	-.348	.095	-.529	.378	-.598	.571	- - -	-.150	- - -	.082	- - -	.359	- - -	.550
	.622	-.188	-.158	-.373	.073	-.668	.377	-.629	.572	-.198	- - -	-.387	- - -	-.530	- - -	-.588	- - -
	.667	-.200	- - -	-.407	- - -	-.711	- - -	-.624	- - -	-.207	-.175	-.397	.073	-.667	.346	-.586	.550
	.711	-.223	- - -	-.485	- - -	-.725	- - -	-.614	- - -	-.216	-.194	-.407	.061	-.664	.374	.585	.567
	.756	-.235	-.202	-.525	.023	-.741	.366	-.617	.596	- - -	-.222	- - -	.046	- - -	.347	- - -	.579
	.800	-.241	-.207	-.551	.029	-.754	.374	-.600	.610	-.241	-.211	-.431	.060	-.720	.370	-.570	.611
	.844	-.238	-.209	-.577	.050	-.778	.387	-.555	.632	-.220	-.185	-.387	.071	-.730	.380	-.548	.621
	.867	- - -	-.209	- - -	.063	- - -	.402	- - -	.651	- - -	-.188	- - -	.085	- - -	.387	- - -	.642
	.889	- - -	-.197	- - -	.083	- - -	.413	- - -	.673	-.165	-.124	-.477	.122	-.732	.415	-.527	.672
	.911	-.207	-.177	-.577	.113	-.790	.445	-.545	.702	-.145	-.071	-.505	.170	-.747	.453	-.526	.703
	.933	-.195	-.146	-.586	.144	-.806	.483	-.537	.734	-.108	-.013	-.514	.229	-.766	.505	-.526	.737
	.956	-.155	-.085	-.584	.216	-.803	.544	-.573	.774	-.010	.055	-.504	.299	-.755	.565	-.499	.795
	.978	-.127	-.026	-.625	.336	-.844	.637	-.546	.818	.056	- - -	-.555	- - -	-.823	- - -	-.484	- - -
	.100	- - -	- - -	- - -	- - -	- - -	- - -	- - -	- - -	- - -	- - -	- - -	- - -	- - -	- - -	- - -	- - -

[1]Flow in tunnel may be choked at these test conditions.

NACA

TABLE II.– CONTINUED

(b) M = 1.30.

Round-nose airfoil											
Station		α=0		α=5.1		α=10.4		α=15.4		α=20.6	
x/c_r	$\frac{y}{s/2}$	P_u	P_l	P_u	P_l	P_u	P_l	P_u	P_l	P_u	P_l
	0	0.012	0.027	-0.116	0.160	-0.203	0.331	-0.366	0.514	-0.342	0.733
	.267	.005	.023	-.134	.162	-.227	.337	-.294	.532	-.370	.746
	.400	.004	.026	-.159	.177	-.247	.355	-.234	.554	-.703	.770
	.533	.007	.029	-.165	.200	-.367	.385	-.566	.584	-.735	.797
0.25	.667	- - -	.044	- - -	.228	- - -	.425	- - -	.629	- - -	.840
	.733	.026	.047	-.245	.259	-.457	.459	-.646	.665	-.771	.874
	.800	.016	.056	-.281	.287	-.493	.498	-.652	.705	-.772	.906
	.867	.040	.090	-.257	.346	-.489	.566	-.672	.768	-.780	.948
	.933	.120	.251	-.203	.508	-.464	.709	-.674	.865	-.774	.990
	.100	- - -	.546	- - -	.734	- - -	.792	- - -	.782	- - -	.715
	0	-.066	-.055	-.188	.081	-.256	.267	-.318	.519	-.412	.690
	.133	-.071	-.051	-.193	.083	-.270	.267	-.336	.514	-.409	.689
	.267	- - -	-.065	- - -	.075	- - -	.246	- - -	.495	- - -	.677
	.400	-.090	-.070	-.227	.078	-.316	.257	-.407	.501	-.696	.685
	.467	-.103	-.074	-.249	.081	-.325	.265	-.526	.505	-.684	.694
	.533	-.103	-.082	-.261	.067	-.442	.272	-.586	.518	-.731	.697
	.600	- - -	-.072	- - -	.087	- - -	.277	- - -	.518	- - -	.719
0.50	.667	-.102	-.082	-.306	.098	-.521	.297	-.639	.538	-.781	.730
	.733	-.090	-.070	-.339	.120	-.542	.321	-.690	.562	-.779	.755
	.800	-.088	-.049	-.373	.161	-.574	.366	-.660	.606	-.780	.790
	.867	-.067	-.036	-.383	.216	-.588	.430	-.671	.661	-.785	.834
	.900	-.052	-.029	-.392	.243	-.607	.465	-.684	.693	-.788	.861
	.933	-.046	.004	-.380	.303	-.618	.534	-.699	.751	-.778	.894
	.967	.054	.104	-.306	.427	-.618	.645	-.711	.824	-.766	.913
	.100	- - -	.576	- - -	.683	- - -	.649	- - -	.566	- - -	.416
	0	- - -	- - -	- - -	- - -	- - -	- - -	- - -	- - -	- - -	- - -
	.177	- - -	- - -	- - -	- - -	- - -	- - -	- - -	- - -	- - -	- - -
	.266	- - -	- - -	- - -	- - -	- - -	- - -	- - -	- - -	- - -	- - -
	.356	- - -	- - -	- - -	- - -	- - -	- - -	- - -	- - -	- - -	- - -
	.446	- - -	-.087	- - -	.045	- - -	.405	- - -	.584	- - -	.631
	.533	-.135	-.116	-.304	.039	-.464	.386	-.474	.516	-.705	.629
	.578	-.143	-.124	-.322	.037	-.528	.382	-.581	.519	-.716	.639
	.622	-.157	-.131	-.342	.036	-.567	.378	-.603	.516	-.731	.633
	.667	-.160	- - -	-.381	- - -	-.581	- - -	-.613	- - -	-.728	- - -
0.75	.711	-.179	- - -	-.407	- - -	-.588	- - -	-.613	- - -	-.721	- - -
	.756	-.190	-.159	-.440	.032	-.606	.323	-.605	.530	-.719	.652
	.800	-.190	-.166	-.459	.044	-.615	.319	-.598	.532	-.708	.664
	.844	-.181	-.165	-.449	.058	-.627	.313	-.607	.546	-.695	.684
	.867	- - -	-.150	- - -	.077	- - -	.324	- - -	.564	- - -	.704
	.889	- - -	-.138	- - -	.097	- - -	.338	- - -	.584	- - -	.720
	.911	-.144	-.114	-.433	.125	-.639	.365	-.598	.607	-.684	.741
	.933	-.128	-.083	-.436	.159	-.652	.413	-.603	.665	-.681	.776
	.956	-.085	-.028	-.427	.232	-.653	.467	-.581	.689	-.683	.799
	.978	-.054	.029	-.464	.342	-.695	.578	-.593	.763	-.664	.826
	.100	- - -	- - -	- - -	- - -	- - -	- - -	- - -	- - -	- - -	- - -

Sharp-nose airfoil									
α=0		α=5.1		α=10.4		α=15.6		α=20.8	
P_u	P_l	P_u	P_l	P_u	P_l	P_u	P_l	P_u	P_l
0.054	0.065	-0.057	0.195	-0.156	0.352	-0.247	0.524	-0.326	0.738
.054	.074	-.073	.224	-.176	.385	-.369	.561	-.280	.772
.073	.100	-.065	.257	-.184	.417	-.332	.597	- 627	.804
.105	.145	-.049	.305	-.184	.468	-.331	.645	-.637	.844
.155	.186	-.029	.346	-.153	.516	-.583	.697	-.747	.886
.190	.226	.007	.385	-.305	.562	-.638	.736	-.775	.921
.229	.286	.025	.456	-.451	.627	-.683	.785	-.781	.957
.288	.355	.087	.536	-.532	.700	-.732	.850	-.778	.995
.387	.406	-.175	.626	-.662	.779	-.740	.901	-.775	1.012
- - -	- - -	- - -	- - -	- - -	- - -	- - -	- - -	- - -	- - -
-.046	-.024	-.150	.095	-.246	.249	-.324	.502	-.403	.677
-.049	-.039	-.161	.092	-.260	.251	-.339	.501	-.407	.676
-.066	-.050	-.181	.100	-.289	.259	-.369	.494	-.421	.682
- - -	-.068	- - -	.092	- - -	.284	- - -	.532	- - -	.693
-.097	-.063	-.233	.115	-.344	.324	-.482	.531	-.688	.707
-.102	-.072	-.238	.094	-.351	.317	-.587	.525	-.702	.704
- - -	-.051	- - -	.117	- - -	.318	- - -	.533	- - -	.724
-.071	-.050	-.230	.122	-.453	.309	-.653	.533	-.754	.727
-.050	-.010	-.224	.166	-.523	.342	-.658	.572	-.750	.765
-.004	.054	-.209	.242	-.538	.413	-.669	.633	-.762	.809
.077	.131	-.129	.330	-.543	.494	-.682	.699	-.767	.860
.108	.183	-.115	.384	-.562	.553	-.699	.743	-.777	.891
.169	.263	-.247	.467	-.594	.636	-.711	.799	-.759	.926
.238	.345	-.391	.579	-.699	.714	-.728	.859	-.775	.940
- - -	- - -	- - -	- - -	- - -	- - -	- - -	- - -	- - -	- - -
- - -	- - -	- - -	- - -	- - -	- - -	- - -	- - -	- - -	- - -
- - -	- - -	- - -	- - -	- - -	- - -	- - -	- - -	- - -	- - -
- - -	- - -	- - -	- - -	- - -	- - -	- - -	- - -	- - -	- - -
- - -	- - -	- - -	- - -	- - -	- - -	- - -	- - -	- - -	- - -
-.127	-.109	-.252	.062	-.367	.381	-.519	.509	-.705	.622
-.143	-.118	-.293	.086	-.396	.365	-.583	.502	-.678	.634
- - -	-.132	- - -	.076	- - -	.357	- - -	.504	- - -	.631
-.170	- - -	-.332	.136	-.485	- - -	-.654	- - -	-.700	- - -
-.172	-.153	-.336	.069	-.577	.332	-.668	.494	-.702	.629
-.168	-.159	-.331	.062	-.578	.300	-.641	.524	-.712	.653
- - -	-.174	- - -	.037	- - -	.274	- - -	.513	- - -	.652
-.175	-.149	-.341	.054	-.600	.288	-.671	.533	-.701	.682
-.154	-.126	-.314	.073	-.606	.304	-.677	.544	-.692	.694
- - -	-.106	- - -	.098	- - -	.315	- - -	.560	- - -	.707
-.098	-.065	-.367	.135	-.603	.345	-.667	.588	- 679	.733
-.070	-.013	-.379	.195	-.606	.393	-.674	.622	-.675	.765
-.034	.045	-.385	.260	-.624	.446	-.689	.673	-.671	.795
.057	.107	-.373	.327	-.613	.509	-.652	.708	-.637	.821
.117	- - -	-.412	- - -	-.683	- - -	-.687	- - -	-.655	- - -
- - -	- - -	- - -	- - -	- - -	- - -	- - -	- - -	- - -	- - -

TABLE II.- CONTINUED

(c) M = 1.40.

Round-nose airfoil												Sharp-nose airfoil									
Station		α=0		α=5.1		α=10.4		α=15.4		α=20.6		α=0		α=5.1		α=10.4		α=15.6		α=20.8	
x/c_r	$\frac{y}{s/2}$	P_u	P_l	P_u	P_l	P_u	P_l	P_u	P_l	P_u	P_l	P_u	P_l	P_u	P_l	P_u	P_l	P_u	P_l	P_u	P_l
	0	0.012	0.025	-0.110	0.150	-0.179	0.306	-0.229	0.480	-0.361	0.659	0.043	0.055	-0.062	0.179	-0.152	0.315	-0.228	0.498	-0.309	0.679
	.267	.011	.022	-.128	.153	-.200	.315	-.254	.496	-.378	.672	.048	.067	-.070	.201	-.170	.361	-.257	.528	-.379	.711
	.400	.011	.030	-.148	.167	-.228	.333	-.306	.516	-.630	.696	.063	.093	-.063	.238	-.171	.406	-.257	.563	-.472	.745
	.533	.012	.032	-.156	.191	-.316	.364	-.478	.552	-.630	.732	.102	.135	-.048	.297	-.173	.452	-.346	.625	-.495	.793
0.25	.667	- - -	.032	- - -	.217	- - -	.411	- - -	.602	- - -	.771	.146	.181	-.021	.344	-.146	.497	-.501	.660	-.647	.838
	.733	.032	.057	-.218	.253	-.396	.444	-.537	.634	.660	.811	.183	.223	.021	.385	-.278	.537	-.531	.705	-.672	.881
	.800	.032	.061	-.231	.281	-.408	.480	-.548	.675	-.666	.842	.231	.282	.044	.456	-.343	.607	-.571	.761	-.679	.922
	.867	.065	.103	-.195	.339	-.397	.545	-.575	.742	-.677	.895	.295	.354	.094	.537	-.393	.683	-.636	.822	-.696	.967
	.933	.142	.262	-.132	.503	-.365	.689	-.572	.852	-.669	.963	.395	.406	-.077	.620	-.532	.763	-.665	.885	-.697	1.003
	.100	- - -	.544	- - -	.734	- - -	.798	- - -	.883	- - -	.751	- - -	- - -	- - -	- - -	- - -	- - -	- - -	- - -	- - -	- - -
	0	-.052	-.046	-.179	.065	-.224	.227	-.278	.438	-.426	.660	-.047	-.035	-.139	.093	-.227	.228	-.305	.405	-.377	.652
	.133	-.063	-.040	-.185	.074	-.238	.243	-.296	.435	-.428	.654	-.054	-.043	-.151	.089	-.240	.236	-.314	.404	-.386	.643
	.267	- - -	-.046	- - -	.066	- - -	.229	- - -	.409	- - -	.643	-.066	-.056	-.174	.085	-.264	.238	-.344	.409	-.439	.649
	.400	-.073	-.054	-.216	.067	-.282	.239	-.364	.419	-.572	.652	- - -	-.073	- - -	.079	- - -	.252	- - -	.449	- - -	.662
	.467	-.081	-.061	-.232	.070	-.305	.249	-.482	.426	-.642	.666	-.095	-.065	-.217	.107	-.312	.293	-.445	.490	-.581	.687
	.533	-.083	-.052	-.247	.060	-.399	.260	-.522	.459	-.667	.643	-.091	-.065	-.220	.083	-.315	.278	-.534	.488	-.654	.678
	.600	- - -	-.066	- - -	.078	- - -	.259	- - -	.451	- - -	.678	- - -	-.042	- - -	.109	- - -	.281	- - -	.511	- - -	.700
0.50	.667	-.081	-.062	-.290	.085	-.444	.280	-.561	.472	-.679	.699	-.058	-.039	-.203	.122	-.415	.287	-.571	.485	-.660	.705
	.733	-.067	-.039	-.310	.112	-.462	.309	-.578	.503	-.684	.728	-.029	-.002	-.195	.166	-.432	.325	-.576	.514	-.680	.740
	.800	-.058	-.029	-.315	.159	-.479	.353	-.588	.549	-.689	.761	.011	.070	-.173	.242	-.439	.404	-.584	.575	-.679	.793
	.867	-.032	-.017	-.310	.211	-.491	.413	-.598	.611	-.693	.822	.095	.144	-.089	.330	-.438	.482	-.598	.650	-.688	.853
	.900	-.026	-.008	-.313	.239	-.503	.458	-.606	.650	-.698	.851	.131	.200	-.073	.384	-.453	.524	-.619	.696	-.698	.887
	.933	-.015	.032	-.297	.295	-.518	.514	-.620	.711	-.699	.894	.179	.274	-.170	.470	-.483	.612	-.641	.760	-.687	.931
	.967	.091	.134	-.219	.419	-.507	.631	-.632	.794	-.705	.925	.265	.356	-.277	.573	-.577	.708	-.675	.831	-.706	.954
	.100	- - -	.582	- - -	.695	- - -	.673	- - -	.618	- - -	.511	- - -	- - -	- - -	- - -	- - -	- - -	- - -	- - -	- - -	- - -
	0	- - -	- - -	- - -	- - -	- - -	- - -	- - -	- - -	- - -	- - -	- - -	- - -	- - -	- - -	- - -	- - -	- - -	- - -	- - -	- - -
	.177	- - -	- - -	- - -	- - -	- - -	- - -	- - -	- - -	- - -	- - -	- - -	- - -	- - -	- - -	- - -	- - -	- - -	- - -	- - -	- - -
	.266	- - -	- - -	- - -	- - -	- - -	- - -	- - -	- - -	- - -	- - -	- - -	- - -	- - -	- - -	- - -	- - -	- - -	- - -	- - -	- - -
	.356	- - -	- - -	- - -	- - -	- - -	- - -	- - -	- - -	- - -	- - -	- - -	- - -	- - -	- - -	- - -	- - -	- - -	- - -	- - -	- - -
	.446	- - -	-.067	- - -	.033	- - -	.287	- - -	.553	- - -	.652	-.119	-.107	-.251	.046	-.341	.211	-.472	.326	-.556	.644
	.533	-.115	-.095	-.285	.036	-.435	.237	-.480	.534	-.653	.653	-.128	-.115	-.281	.066	-.357	.220	-.549	.315	-.624	.647
	.578	-.114	-.104	-.300	.030	-.459	.242	-.530	.533	-.655	.650	- - -	-.127	- - -	.065	- - -	.225	- - -	.307	- - -	.647
	.622	-.124	-.119	-.323	.035	-.476	.238	-.553	.523	-.666	.655	-.148	- - -	-.299	.066	-.472	- - -	-.594	- - -	-.636	- - -
	.667	-.129	- - -	-.345	- - -	-.488	- - -	-.556	- - -	-.672	- - -	-.148	-.135	-.304	.043	-.493	.231	-.603	.494	-.634	.654
0.75	.711	-.145	- - -	-.364	.064	-.502	- - -	-.565	- - -	-.674	- - -	-.139	-.132	-.303	.043	-.494	.266	-.590	.519	-.636	.681
	.756	-.148	-.122	-.389	.037	-.515	.257	-.558	.537	-.665	.673	- - -	-.138	- - -	.030	- - -	.241	- - -	.516	- - -	.671
	.800	-.146	-.124	-.385	.048	-.526	.258	-.555	.530	-.663	.682	-.135	-.113	-.293	.057	-.510	.269	-.614	.535	-.632	.698
	.844	-.133	-.117	-.375	.069	-.533	.280	-.572	.547	-.660	.708	-.104	-.080	-.262	.088	-.510	.288	-.619	.538	-.623	.708
	.867	- - -	-.103	- - -	.083	- - -	.298	- - -	.558	- - -	.718	- - -	-.058	- - -	.116	- - -	.306	- - -	.549	- - -	.726
	.889	- - -	-.092	- - -	.107	- - -	.323	- - -	.577	- - -	.737	-.051	-.017	-.292	.157	-.494	.338	-.617	.576	-.620	.747
	.911	-.092	-.072	-.352	.137	-.542	.353	-.571	.607	-.650	.761	-.023	.031	-.300	.213	-.498	.388	-.630	.617	-.617	.777
	.933	-.072	-.030	-.351	.178	-.552	.413	-.578	.661	-.643	.787	.010	.087	-.299	.278	-.528	.446	-.639	.656	-.612	.816
	.956	-.031	.018	-.339	.249	-.556	.461	-.560	.687	-.643	.827	.102	.144	-.281	.352	-.507	.504	-.618	.708	-.580	.841
	.978	.004	.074	-.370	.358	-.594	.570	-.573	.767	-.650	.863	.160	- - -	-.321	- - -	-.569	- - -	-.699	- - -	-.602	- - -
	.100	- - -	- - -	- - -	- - -	- - -	- - -	- - -	- - -	- - -	- - -	- - -	- - -	- - -	- - -	- - -	- - -	- - -	- - -	- - -	- - -

TABLE II.- CONTINUED

(d) M = 1.53.

Round-nose airfoil												Sharp-nose airfoil									
Station		α=0		α=5.1		α=10.4		α=15.4		α=20.6		α=0		α=5.1		α=10.4		α=15.6		α=20.8	
x/c_r	y/(y/2)	P_u	P_l	P_u	P_l	P_u	P_l	P_u	P_l	P_u	P_l	P_u	P_l	P_u	P_l	P_u	P_l	P_u	P_l	P_u	P_l
	0	0.021	0.029	-0.090	0.142	-0.152	0.285	-0.207	0.441	-0.299	0.606	0.044	0.060	-0.055	0.215	-0.131	0.311	-0.206	0.460	-0.268	0.623
	.267	.019	.027	-.105	.142	-.169	.292	-.219	.453	-.294	.618	.048	.064	-.063	.184	-.145	.338	-.228	.498	-.292	.661
	.400	.022	.031	-.120	.156	-.199	.314	-.318	.478	-.488	.643	.072	.092	-.052	.202	-.145	.379	-.231	.540	-.368	.699
	.533	.024	.033	-.139	.174	-.254	.346	-.371	.514	-.497	.683	.098	.127	-.040	.277	-.144	.431	-.334	.590	-.476	.749
0.25	.667	.024	.039	- - -	.201	- - -	.390	- - -	.567	- - -	.729	.144	.179	-.004	.332	-.164	.488	-.391	.635	-.504	.794
	.733	.041	.063	-.170	.239	-.310	.428	-.423	.603	-.587	.764	.186	.219	.033	.378	-.212	.527	-.401	.677	-.522	.837
	.800	.046	.077	-.171	.267	-.306	.463	-.430	.637	-.526	.799	.231	.278	.058	.448	-.241	.595	-.434	.738	-.541	.887
	.867	.096	.125	-.124	.327	-.289	.526	-.442	.703	-.535	.855	.297	.346	.107	.531	-.275	.667	-.482	.809	-.572	.943
	.933	.167	.286	-.065	.495	-.247	.669	-.434	.826	-.526	.943	.401	.394	.054	.615	-.385	.741	-.537	.875	-.586	.987
	.100	- - -	.559	- - -	.718	- - -	.790	- - -	.823	- - -	.806	- - -	- - -	- - -	- - -	- - -	- - -	- - -	- - -	- - -	- - -
	0	-.038	-.037	-.146	.069	-.191	.201	-.229	.367	-.346	.572	-.041	-.027	-.126	.084	-.192	.213	-.266	.351	-.324	.552
	.133	-.047	-.033	-.148	.071	-.207	.221	-.249	.383	-.352	.558	-.047	-.036	-.134	.085	-.201	.220	-.279	.361	-.331	.547
	.267	- - -	-.040	- - -	.068	- - -	.211	- - -	.375	- - -	.539	-.060	-.049	-.156	.081	-.229	.218	-.302	.370	-.350	.555
	.400	-.060	-.046	-.179	.069	-.245	.229	-.353	.390	-.498	.552	- - -	-.062	- - -	.078	- - -	.230	- - -	.397	- - -	.598
	.467	-.070	-.051	-.192	.077	-.300	.237	-.405	.408	-.584	.571	-.074	-.048	-.190	.095	-.272	.277	-.397	.440	-.508	.640
	.533	-.070	-.044	-.203	.076	-.329	.246	-.423	.421	-.531	.578	-.071	-.049	-.185	.094	-.270	.264	-.447	.444	-.525	.621
	.600	- - -	-.054	- - -	.085	- - -	.247	- - -	.425	- - -	.592	- - -	-.021	- - -	.128	- - -	.289	- - -	.480	- - -	.651
0.50	.667	-.065	-.045	-.246	.100	-.365	.268	-.455	.446	-.544	.621	-.028	-.010	-.165	.134	-.335	.280	-.467	.448	-.544	.629
	.733	-.044	-.031	-.241	.130	-.365	.301	-.466	.483	-.551	.655	.004	.027	-.149	.174	-.333	.325	-.467	.492	-.546	.663
	.800	-.029	-.016	-.231	.168	-.375	.346	-.477	.528	-.561	.705	.043	.097	-.126	.252	-.337	.404	-.476	.557	-.557	.728
	.867	-.003	.003	-.220	.222	-.377	.410	-.486	.591	-.565	.770	.121	.169	-.048	.341	-.331	.491	-.486	.637	-.573	.799
	.900	.006	.023	-.218	.251	-.384	.444	-.488	.630	-.568	.800	.161	.224	-.033	.402	-.349	.542	-.503	.683	-.587	.840
	.933	.027	.063	-.198	.306	-.391	.509	-.509	.691	-.580	.854	.211	.293	-.078	.486	-.363	.616	-.527	.751	-.582	.890
	.967	.034	.171	-.118	.426	-.380	.621	-.519	.782	-.589	.913	.291	.375	-.158	.592	-.449	.711	-.577	.829	-.609	.934
	.100	- - -	.602	- - -	.716	- - -	.696	- - -	.661	- - -	.593	- - -	- - -	- - -	- - -	- - -	- - -	- - -	- - -	- - -	- - -
	0	- - -	- - -	- - -	- - -	- - -	- - -	- - -	- - -	- - -	- - -	- - -	- - -	- - -	- - -	- - -	- - -	- - -	- - -	- - -	- - -
	.177	- - -	- - -	- - -	- - -	- - -	- - -	- - -	- - -	- - -	- - -	- - -	- - -	- - -	- - -	- - -	- - -	- - -	- - -	- - -	- - -
	.266	- - -	- - -	- - -	- - -	- - -	- - -	- - -	- - -	- - -	- - -	- - -	- - -	- - -	- - -	- - -	- - -	- - -	- - -	- - -	- - -
	.356	- - -	- - -	- - -	- - -	- - -	- - -	- - -	- - -	- - -	- - -	- - -	- - -	- - -	- - -	- - -	- - -	- - -	- - -	- - -	- - -
	.446	- - -	-.068	- - -	.055	- - -	.203	- - -	.467	- - -	.680	-.107	-.099	-.220	.066	-.314	.188	-.425	.368	-.519	.670
	.533	-.101	-.087	-.235	.056	-.357	.206	-.419	.403	-.536	.673	-.114	-.098	-.237	.066	-.317	.213	-.467	.369	-.589	.662
	.578	-.106	-.095	-.257	.048	-.369	.216	-.446	.406	-.543	.671	- - -	-.109	- - -	.065	- - -	.216	- - -	.377	- - -	.665
	.622	-.114	-.098	-.268	.051	-.380	.221	-.460	.402	-.554	.668	-.130	- - -	-.256	- - -	-.401	- - -	-.501	- - -	.547	- - -
	.667	-.114	- - -	-.288	- - -	-.396	- - -	-.470	- - -	-.561	- - -	-.122	-.107	-.255	.055	-.409	.229	-.507	.405	.559	.658
0.75	.711	-.127	- - -	-.299	- - -	-.409	- - -	-.479	- - -	-.562	- - -	-.109	-.099	-.244	.053	-.402	.253	-.500	.446	-.557	.689
	.756	-.121	-.099	-.299	.058	-.419	.244	-.471	.439	-.558	.688	- - -	-.100	- - -	.054	- - -	.220	- - -	.420	- - -	.680
	.800	-.111	-.095	-.296	.070	-.421	.256	-.487	.441	-.557	.682	-.089	-.071	-.229	.089	-.416	.254	-.516	.458	-.572	.709
	.844	-.092	-.090	-.283	.095	-.429	.280	-.492	.468	-.564	.701	-.064	-.055	-.198	.127	-.412	.276	-.521	.478	-.571	.711
	.867	- - -	-.067	- - -	.113	- - -	.302	- - -	.488	- - -	.716	- - -	-.011	- - -	.156	- - -	.301	- - -	.498	- - -	.727
	.889	- - -	-.054	- - -	.137	- - -	.325	- - -	.512	- - -	.734	-.001	.031	-.207	.196	-.407	.346	-.522	.528	-.572	.752
	.911	-.043	-.032	-.253	.168	-.433	.358	-.498	.543	-.562	.759	.029	.080	-.212	.256	-.405	.397	-.528	.570	-.572	.786
	.933	-.028	.015	-.244	.217	-.438	.415	-.503	.607	-.561	.789	.065	.189	-.208	.316	-.412	.458	-.537	.619	-.571	.826
	.956	.017	.057	-.231	.286	-.446	.469	-.496	.698	-.563	.832	.146	.189	-.184	.387	-.403	.524	-.528	.669	-.537	.859
	.978	.059	.117	-.256	.387	-.480	.571	-.513	.737	-.564	.884	.210	- - -	-.208	- - -	-.432	- - -	-.577	- - -	-.577	- - -
	.100	- - -	- - -	- - -	- - -	- - -	- - -	- - -	- - -	- - -	- - -	- - -	- - -	- - -	- - -	- - -	- - -	- - -	- - -	- - -	- - -

TABLE II.- CONTINUED

(e) M = 1.60.

Round-nose airfoil												Sharp-nose airfoil									
Station		α=0		α=5.1		α=10.4		α=15.4		α=20.6		α=0		α=5.1		α=10.4		α=15.6		α=20.8	
x/c_r	$\frac{y}{w/2}$	P_u	P_l	P_u	P_l	P_u	P_l	P_u	P_l	P_u	P_l	P_u	P_l	P_u	P_l	P_u	P_l	P_u	P_l	P_u	P_l
	0	0.023	0.030	-0.082	0.130	-0.150	0.271	-0.188	0.430	-0.282	0.588	0.038	0.052	-0.058	0.158	-0.126	0.296	-0.186	0.450	-0.245	0.641
	.267	.020	.031	-.095	.136	-.164	.277	-.197	.444	-.260	.599	.044	.059	-.061	.173	-.137	.324	-.207	.483	-.267	.648
	.400	.024	.033	-.110	.149	-.199	.303	-.317	.474	-.425	.620	.064	.092	-.054	.212	-.135	.369	-.218	.526	-.348	.682
	.533	.027	.034	-.122	.154	-.238	.332	-.336	.502	-.437	.660	.096	.123	-.038	.260	-.136	.428	-.302	.581	-.418	.735
0.25	.667	- - -	.041	- - -	.186	- - -	.376	- - -	.553	- - -	.709	.142	.176	-.003	.319	-.160	.479	-.338	.626	-.435	.781
	.733	.049	.070	-.140	.230	-.280	.418	-.377	.593	-.463	.748	.182	.214	.030	.363	-.176	.522	-.348	.664	-.452	.823
	.800	.051	.086	-.136	.255	-.271	.450	-.380	.629	-.461	.781	.228	.273	.059	.428	-.194	.591	-.371	.728	-.463	.874
	.867	.107	.134	-.094	.320	-.251	.513	-.387	.688	-.464	.838	.298	.336	.101	.512	-.220	.666	-.416	.792	-.495	.930
	.933	.180	.298	-.032	.487	-.204	.660	-.380	.808	-.454	.933	.394	.394	.078	.601	-.305	.743	-.474	.858	-.521	.976
	.100	- - -	.556	- - -	.716	- - -	.788	- - -	.818	- - -	.819	- - -	- - -	- - -	- - -	- - -	- - -	- - -	- - -	- - -	- - -
	0	-.031	-.031	-.145	.062	-.185	.198	-.217	.355	-.321	.538	-.030	-.021	-.114	.091	-.185	.211	-.241	.343	-.301	.520
	.133	-.039	-.030	-.149	.068	-.199	.212	-.231	.375	-.330	.538	-.035	-.025	-.126	.065	-.195	.209	-.254	.349	-.310	.528
	.267	- - -	-.042	- - -	.059	- - -	.199	- - -	.359	- - -	.535	-.053	-.043	-.148	.077	-.221	.204	-.283	.349	-.325	.544
	.400	-.057	-.047	-.178	.063	-.256	.214	-.346	.379	-.458	.555	- - -	-.060	- - -	.067	- - -	.206	- - -	.374	- - -	.592
	.467	-.068	-.049	-.193	.063	-.297	.224	-.378	.392	-.468	.573	-.075	-.045	-.180	.087	-.265	.256	-.380	.422	-.459	.652
	.533	-.065	-.040	-.206	.060	-.311	.230	-.389	.414	-.472	.570	-.063	-.049	-.173	.085	-.269	.243	-.412	.432	-.471	.655
	.600	- - -	-.051	- - -	.075	- - -	.239	- - -	.429	- - -	.599	- - -	-.015	- - -	.119	- - -	.273	- - -	.470	- - -	.685
0.50	.667	-.058	-.042	-.237	.090	-.342	.264	-.418	.457	-.486	.629	-.020	-.004	-.152	.128	-.309	.270	.420	.448	-.485	.659
	.733	-.035	-.026	-.223	.122	-.336	.296	-.425	.493	-.494	.661	.009	.034	-.134	.176	-.302	.318	.418	.496	-.482	.687
	.800	-.019	-.001	-.206	.165	-.335	.355	-.435	.545	-.504	.714	.051	.103	-.105	.255	-.299	.402	.424	.574	-.491	.749
	.867	.013	.019	-.195	.223	-.335	.425	-.445	.608	-.507	.775	.134	.179	-.032	.343	-.290	.495	.431	.657	-.505	.821
	.900	.032	.052	-.181	.252	-.338	.462	-.457	.650	-.513	.812	.180	.236	-.020	.406	-.296	.554	.450	.711	-.518	.865
	.933	.057	.100	-.158	.317	-.338	.531	-.463	.711	-.519	.864	.234	.310	-.038	.492	-.309	.639	.468	.781	-.522	.915
	.967	.171	.209	-.077	.440	-.318	.650	-.470	.811	-.530	.930	.315	.399	-.098	.601	-.385	.736	.528	.861	-.551	.969
	.100	- - -	.640	- - -	.745	- - -	.741	- - -	.711	- - -	.640	- - -	- - -	- - -	- - -	- - -	- - -	- - -	- - -	- - -	- - -
	0	- - -	- - -	- - -	- - -	- - -	- - -	- - -	- - -	- - -	- - -	- - -	- - -	- - -	- - -	- - -	- - -	- - -	- - -	- - -	- - -
	.177	- - -	- - -	- - -	- - -	- - -	- - -	- - -	- - -	- - -	- - -	- - -	- - -	- - -	- - -	- - -	- - -	- - -	- - -	- - -	- - -
	.266	- - -	- - -	- - -	- - -	- - -	- - -	- - -	- - -	- - -	- - -	- - -	- - -	- - -	- - -	- - -	- - -	- - -	- - -	- - -	- - -
	.356	- - -	- - -	- - -	- - -	- - -	- - -	- - -	- - -	- - -	- - -	- - -	- - -	- - -	- - -	- - -	- - -	- - -	- - -	- - -	- - -
	.446	- - -	-.052	- - -	.059	- - -	.216	- - -	.420	- - -	.680	- - -	-.062	-.202	.068	-.275	.217	-.392	.367	-.466	.683
	.533	-.084	-.074	-.222	.067	-.333	.223	-.394	.396	-.486	.669	-.086	-.071	-.214	.081	-.301	.232	-.422	.386	-.467	.670
	.578	-.086	-.074	-.240	.071	-.337	.226	-.407	.400	-.485	.669	- - -	-.065	- - -	.077	- - -	.238	- - -	.394	- - -	.669
	.622	-.094	-.078	-.255	.066	-.349	.232	-.424	.405	-.491	.669	-.096	- - -	-.224	- - -	-.346	- - -	-.448	- - -	-.488	- - -
	.667	-.096	- - -	-.258	- - -	-.365	- - -	-.427	- - -	-.504	- - -	-.087	-.076	-.222	.081	-.354	.241	-.452	.421	-.497	.657
0.75	.711	-.101	- - -	-.268	- - -	-.369	- - -	-.439	- - -	-.503	- - -	-.076	-.066	-.216	.082	-.352	.270	-.450	.460	-.493	.680
	.756	-.099	-.079	-.269	.069	-.378	.252	-.438	.449	-.499	.683	- - -	-.064	- - -	.078	- - -	.239	- - -	.429	- - -	.681
	.800	-.090	-.071	-.260	.085	-.380	.267	-.440	.451	-.500	.679	-.064	-.034	-.193	.115	-.364	.268	-.462	.469	-.509	.708
	.844	-.070	-.060	-.249	.108	-.383	.289	-.455	.479	-.509	.699	-.026	.003	-.166	.149	-.361	.289	-.470	.491	-.513	.710
	.867	- - -	-.042	- - -	.128	- - -	.317	- - -	.498	- - -	.710	.007	.026	- - -	.178	- - -	.317	- - -	.507	- - -	.723
	.889	- - -	-.029	- - -	.152	- - -	.339	- - -	.516	- - -	.730	.035	.066	-.165	.203	-.350	.376	-.470	.542	-.510	.752
	.911	-.016	-.004	-.214	.187	-.383	.382	-.463	.557	-.501	.757	.063	.108	-.166	.277	-.350	.416	-.471	.585	-.515	.784
	.933	-.001	.042	-.204	.225	-.387	.427	-.466	.617	-.503	.782	.096	.162	-.161	.341	-.351	.481	-.478	.637	-.523	.825
	.956	.047	.086	-.185	.301	-.389	.486	-.464	.665	-.503	.836	.186	.225	-.139	.408	-.343	.548	-.469	.690	-.486	.865
	.978	.094	.151	-.205	.404	-.417	.595	-.482	.747	-.514	.888	.239	- - -	-.154	- - -	-.386	- - -	-.523	- - -	-.524	- - -
	.100	- - -	- - -	- - -	- - -	- - -	- - -	- - -	- - -	- - -	- - -	- - -	- - -	- - -	- - -	- - -	- - -	- - -	- - -	- - -	- - -

TABLE II.- CONCLUDED

(f) M = 1.70.

Round-nose airfoil												Sharp-nose airfoil									
Station		α=0		α=5.1		α=10.4		α=15.4		α=20.6		α=0		α=5.1		α=10.4		α=15.6		α=20.8	
x/c_r	$\frac{y}{y/2}$	P_u	P_l	P_u	P_l	P_u	P_l	P_u	P_l	P_u	P_l	P_u	P_l	P_u	P_l	P_u	P_l	P_u	P_l	P_u	P_l
	0	0.023	0.032	-0.066	0.122	-0.138	0.261	-0.172	0.409	-0.240	0.568	0.041	0.051	-0.050	0.185	-0.119	0.280	-0.169	0.429	-0.213	0.583
	.267	.021	.029	-.079	.128	-.152	.269	-.173	.422	-.217	.583	.047	.058	-.057	.207	-.129	.306	-.183	.463	-.227	.623
	.400	.026	.035	-.083	.138	-.186	.290	-.262	.446	-.345	.605	.065	.084	-.050	.234	-.133	.345	-.203	.501	-.278	.661
	.533	.027	.036	-.103	.157	-.216	.324	-.285	.485	-.361	.646	.093	.120	-.035	.268	-.132	.401	-.264	.564	-.330	.719
0.25	.667	- - -	.044	- - -	.179	- - -	.364	- - -	.535	- - -	.702	.140	.178	.001	.302	-.138	.462	-.285	.619	-.340	.759
	.733	.053	.072	-.106	.218	-.238	.405	-.319	.582	-.388	.737	.181	.212	.031	.340	-.144	.506	-.287	.654	-.354	.801
	.800	.064	.092	-.088	.243	-.228	.441	-.318	.617	-.382	.771	.226	.266	.057	.410	-.152	.570	-.308	.720	-.363	.852
	.867	.120	.141	-.051	.311	-.205	.503	-.319	.680	-.387	.826	.294	.331	.091	.493	-.167	.650	-.339	.790	-.389	.916
	.933	.189	.299	.010	.473	-.161	.652	-.307	.799	-.370	.920	.389	.382	.103	.578	-.232	.728	-.405	.850	-.428	.960
	.100	- - -	.548	- - -	.700	- - -	.789	- - -	.831	- - -	.831	- - -	- - -	- - -	- - -	- - -	- - -	- - -	- - -	- - -	- - -
	0	-.023	-.023	-.111	.062	-.181	.194	-.199	.336	-.263	.489	-.028	-.016	-.115	.081	-.165	.203	-.222	.328	-.256	.482
	.133	-.027	-.019	-.117	.059	-.186	.209	-.208	.355	-.275	.493	-.036	-.024	-.124	.077	-.179	.208	-.235	.343	-.259	.498
	.267	- - -	-.028	- - -	.061	- - -	.218	- - -	.350	- - -	.501	-.048	-.038	-.142	.072	-.203	.204	-.250	.350	-.277	.506
	.400	-.043	-.032	-.143	.067	-.257	.215	-.313	.367	-.387	.518	- - -	-.052	- - -	.064	- - -	.209	- - -	.358	- - -	.519
	.467	-.051	-.038	-.156	.073	-.273	.222	-.335	.374	-.395	.536	-.058	-.060	-.169	.096	-.239	.251	-.341	.413	-.376	.582
	.533	-.050	-.028	-.166	.062	-.287	.223	-.340	.391	-.398	.542	-.050	-.033	-.166	.085	-.246	.248	-.363	.411	-.382	.582
	.600	- - -	-.040	- - -	.079	- - -	.232	- - -	.402	- - -	.568	- - -	-.004	- - -	.116	- - -	.279	- - -	.459	- - -	.628
0.50	.667	-.043	-.033	-.183	.092	-.308	.255	-.369	.426	-.418	.597	-.012	.004	-.142	.125	-.263	.270	-.368	.431	-.398	.602
	.773	-.021	.005	-.167	.120	-.303	.287	-.367	.460	-.423	.628	.023	.042	-.123	.168	-.259	.318	-.365	.475	-.395	.638
	.800	-.007	.007	-.158	.153	-.297	.335	-.377	.512	-.428	.681	.062	.108	-.089	.241	-.255	.392	-.367	.548	-.401	.709
	.867	.030	.040	-.141	.211	-.291	.401	-.382	.580	-.429	.745	.141	.179	-.027	.329	-.242	.484	-.374	.636	-.409	.776
	.900	.045	.060	-.133	.239	-.291	.436	-.390	.618	-.439	.778	.179	.235	-.011	.391	-.243	.539	-.389	.681	-.420	.820
	.933	.069	.104	-.118	.298	-.286	.499	-.401	.678	-.446	.832	.228	.304	-.009	.475	-.255	.617	-.410	.749	-.436	.877
	.967	.180	.209	-.034	.409	-.263	.618	-.403	.777	-.452	.900	.313	.384	-.049	.578	-.320	.725	-.467	.827	-.472	.936
	.100	- - -	.604	- - -	.706	- - -	.718	- - -	.767	- - -	.637	- - -	- - -	- - -	- - -	- - -	- - -	- - -	- - -	- - -	- - -
	0	- - -	- - -	- - -	- - -	- - -	- - -	- - -	- - -	- - -	- - -	- - -	- - -	- - -	- - -	- - -	- - -	- - -	- - -	- - -	- - -
	.177	- - -	- - -	- - -	- - -	- - -	- - -	- - -	- - -	- - -	- - -	- - -	- - -	- - -	- - -	- - -	- - -	- - -	- - -	- - -	- - -
	.266	- - -	- - -	- - -	- - -	- - -	- - -	- - -	- - -	- - -	- - -	- - -	- - -	- - -	- - -	- - -	- - -	- - -	- - -	- - -	- - -
	.356	- - -	- - -	- - -	- - -	- - -	- - -	- - -	- - -	- - -	- - -	- - -	- - -	- - -	- - -	- - -	- - -	- - -	- - -	- - -	- - -
	.446	- - -	-.052	- - -	.045	- - -	.192	- - -	.355	- - -	.602	- - -	-.069	-.205	.051	-.271	.186	-.366	.328	-.382	.561
	.533	-.080	-.070	-.190	.050	-.304	.207	-.352	.358	-.420	.560	-.092	-.081	-.218	.049	-.291	.207	-.386	.354	-.383	.519
	.578	-.082	-.072	-.202	.052	-.313	.208	-.360	.367	-.418	.546	- - -	-.084	- - -	.054	- - -	.209	- - -	.362	- - -	.527
	.622	-.085	-.073	-.213	.035	-.327	.214	-.374	.374	-.430	.544	-.102	- - -	-.219	- - -	-.323	- - -	-.410	- - -	-.410	- - -
	.667	-.087	- - -	-.216	- - -	-.337	- - -	-.385	- - -	-.437	- - -	-.092	-.077	-.214	.057	-.326	.220	-.416	.384	-.420	.543
0.75	.711	-.091	- - -	-.219	- - -	-.347	- - -	-.392	- - -	-.439	- - -	-.072	-.067	-.213	.059	-.321	.249	-.409	.431	-.417	.519
	.756	-.082	-.068	-.210	.055	-.342	.239	-.390	.420	-.436	.569	- - -	-.063	- - -	.060	- - -	.219	- - -	.399	- - -	.562
	.800	-.072	-.064	-.202	.075	-.342	.250	-.393	.423	-.434	.576	-.049	-.031	-.184	.098	-.328	.247	-.421	.438	-.435	.610
	.844	-.060	-.052	.194	.097	-.341	.279	-.405	.453	-.444	.607	-.019	.009	-.160	.142	-.324	.285	-.423	.457	-.438	.624
	.867	- - -	-.031	- - -	.122	- - -	.305	- - -	.477	- - -	.627	- - -	.032	- - -	.166	- - -	.312	- - -	.477	- - -	.645
	.889	- - -	-.020	- - -	.139	- - -	.326	- - -	.504	- - -	.654	.041	.066	-.145	.209	-.316	.354	-.419	.516	-.434	.676
	.911	-.002	.012	-.159	.168	-.336	.361	-.412	.536	-.442	.684	.074	.114	-.141	.262	-.310	.405	-.423	.563	-.442	.711
	.933	.017	.057	-.150	.205	-.339	.412	-.419	.595	-.444	.725	.105	.164	-.133	.323	-.311	.466	-.435	.614	-.447	.760
	.956	.066	.103	-.119	.287	-.337	.475	-.415	.636	-.444	.773	.188	.224	-.114	.392	-.299	.536	-.424	.665	-.423	.805
	.978	.112	.162	-.136	.384	-.360	.577	-.435	.729	-.464	.845	.246	- - -	-.118	- - -	-.334	- - -	-.473	- - -	-.456	- - -
	.100	- - -	- - -	- - -	- - -	- - -	- - -	- - -	- - -	- - -	- - -	- - -	- - -	- - -	- - -	- - -	- - -	- - -	- - -	- - -	- - -

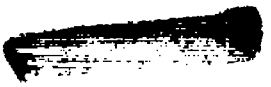

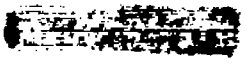

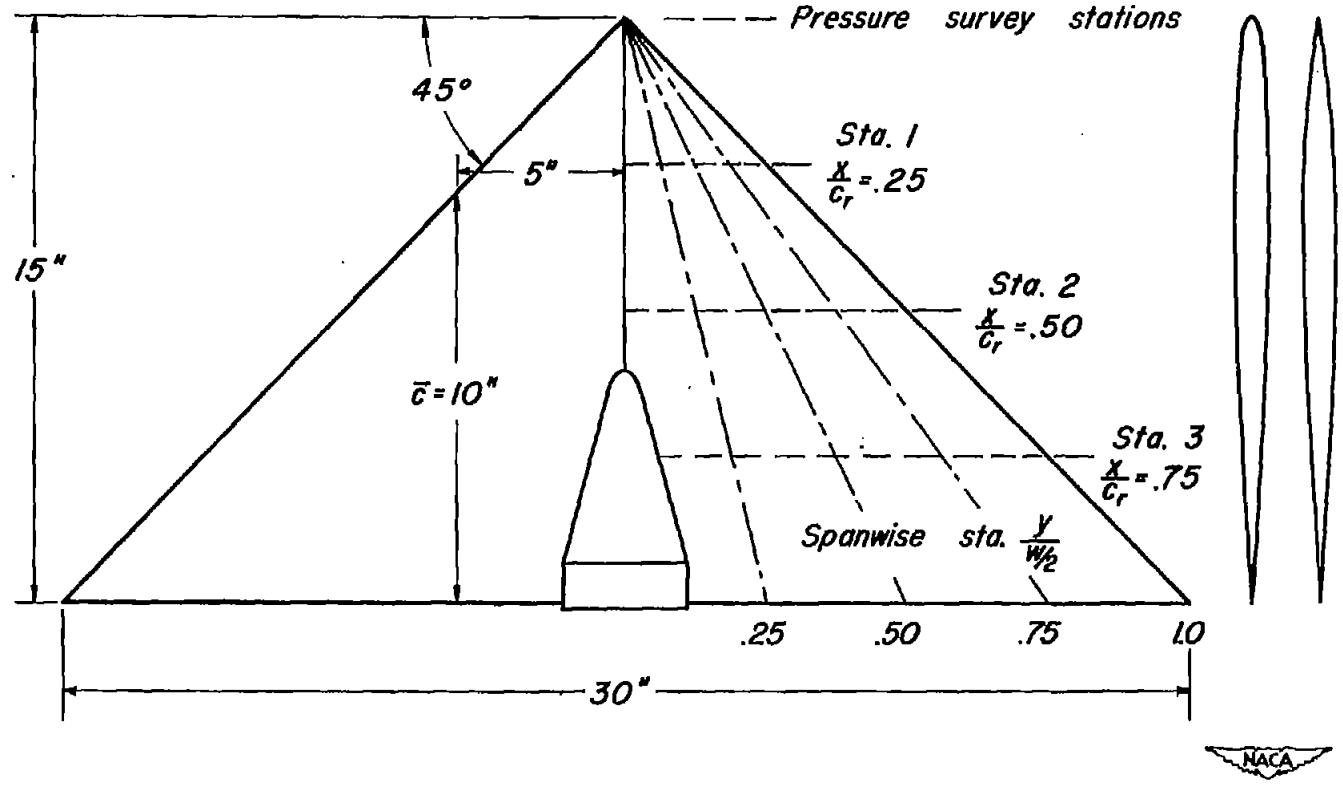

Figure 1.– Dimensional sketch of triangular wing showing both the round-nose airfoil section (NACA 0006-63) and the sharp-nose airfoil section.

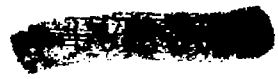

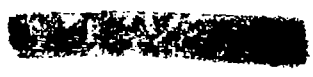

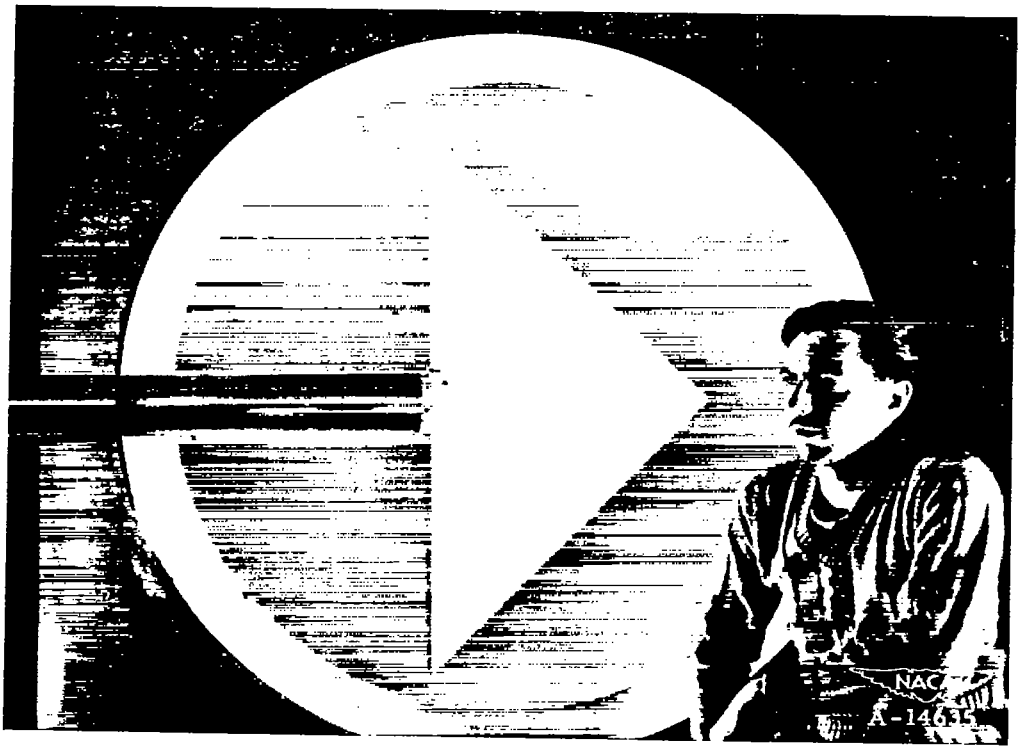

Figure 2.— Model mounted in the Ames 6- by 6-foot supersonic wind tunnel.

[redacted]

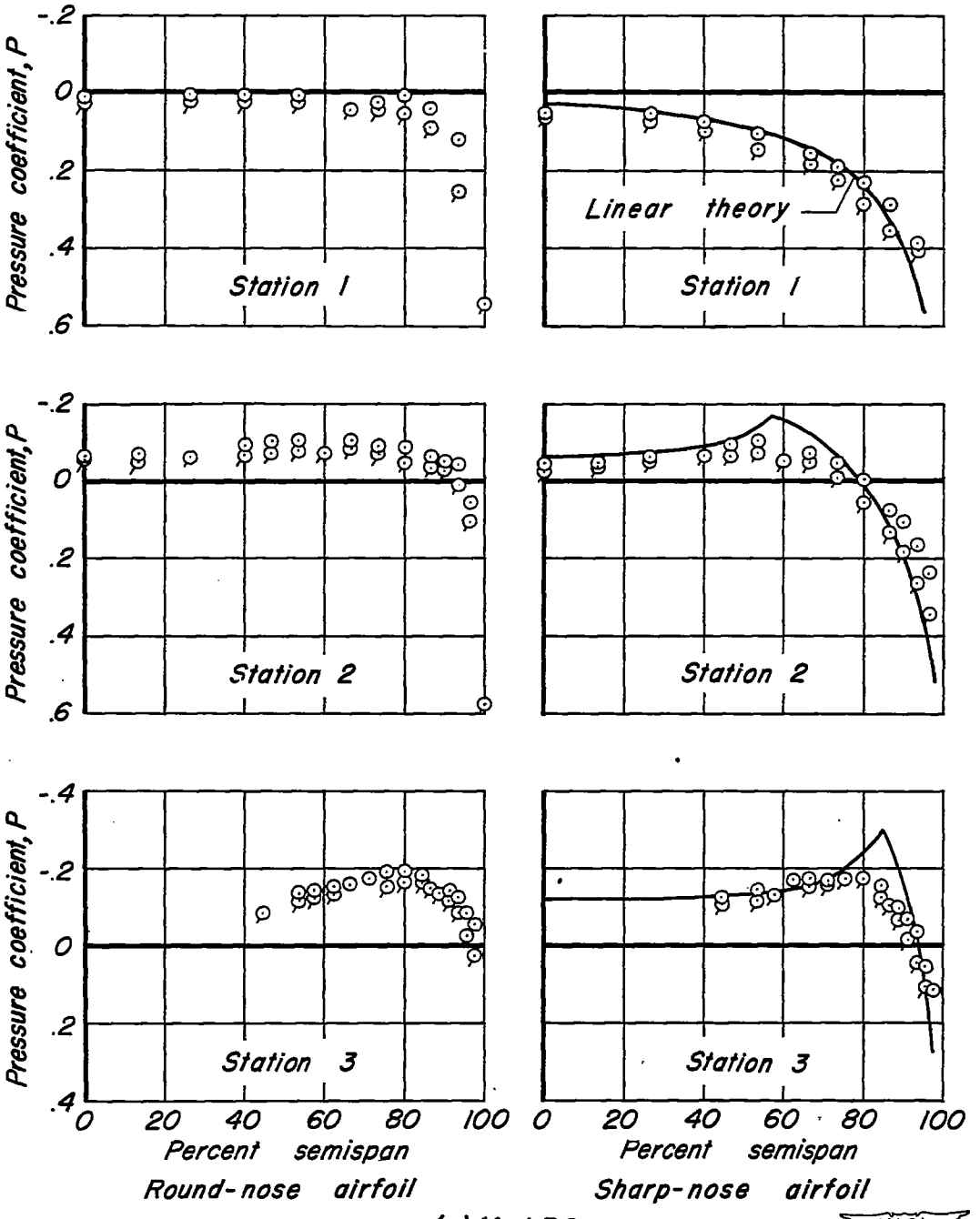

(a) M = 1.30.

NACA

Figure 3.- Comparison of experimental and theoretical pressure distributions for zero angle of attack. Flagged symbols denote lower surface.

[redacted]

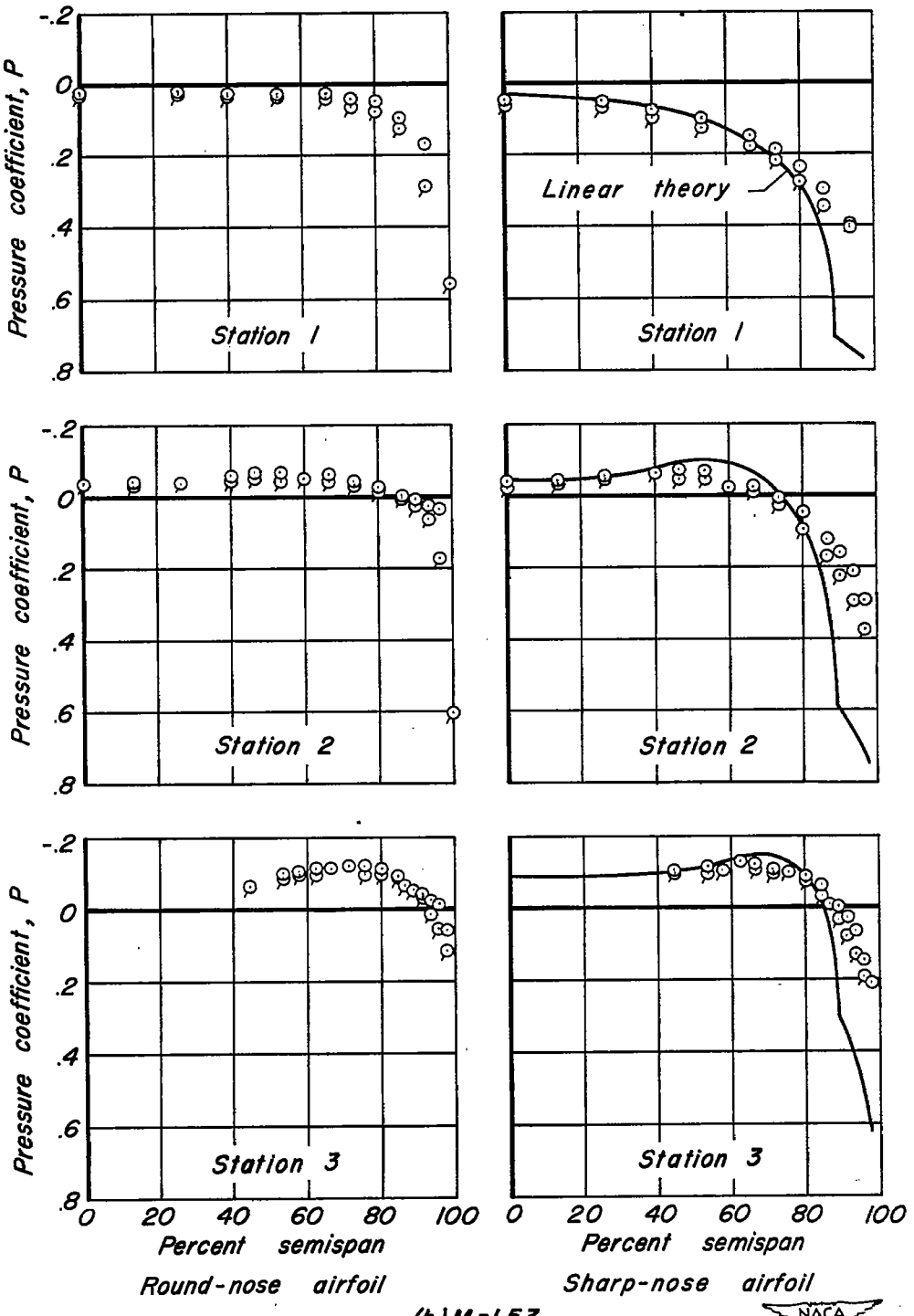

(b) M = 1.53.

Figure 3.- Continued.

[redacted]

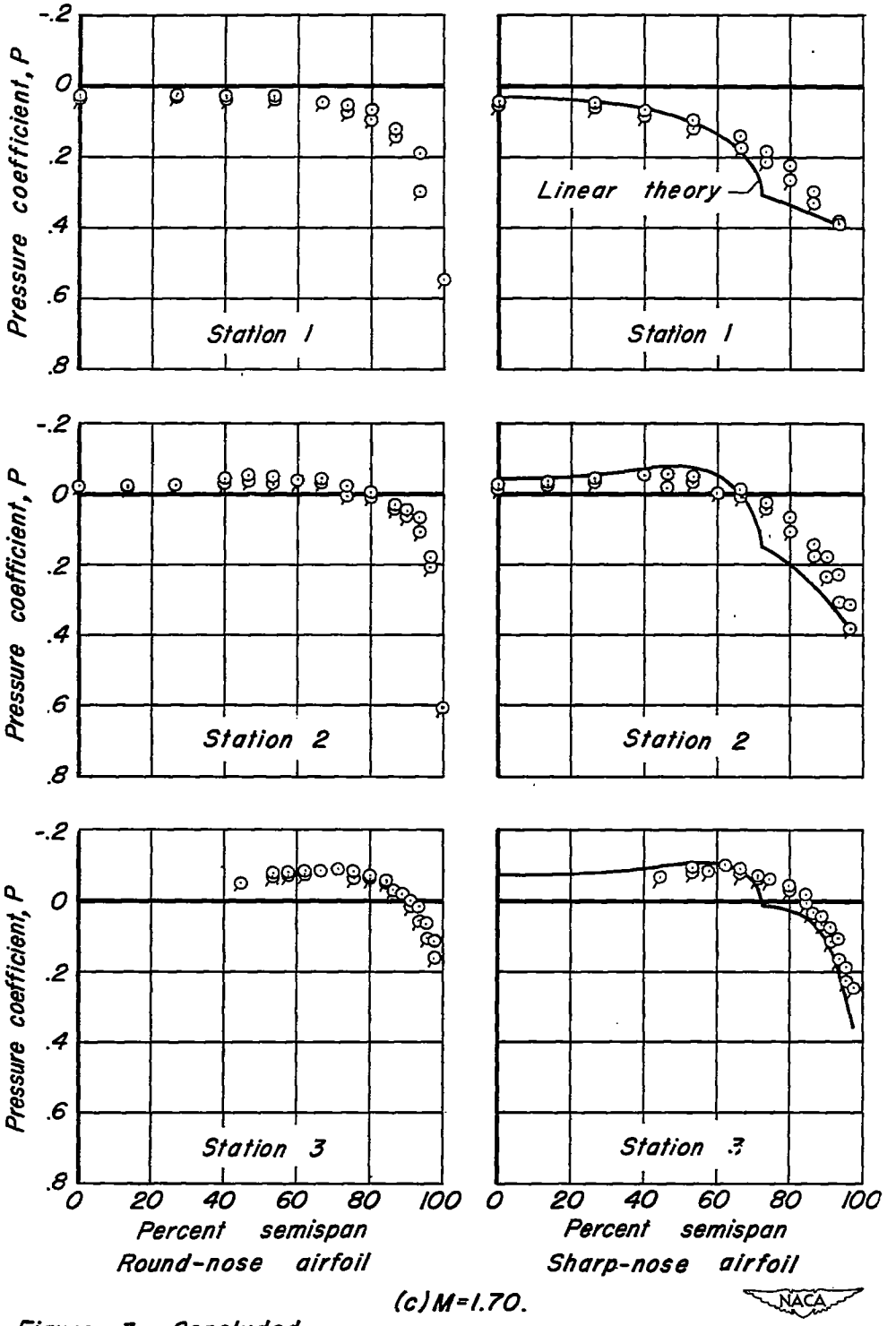

(c) M=1.70.

Figure 3.- Concluded.

[redacted]

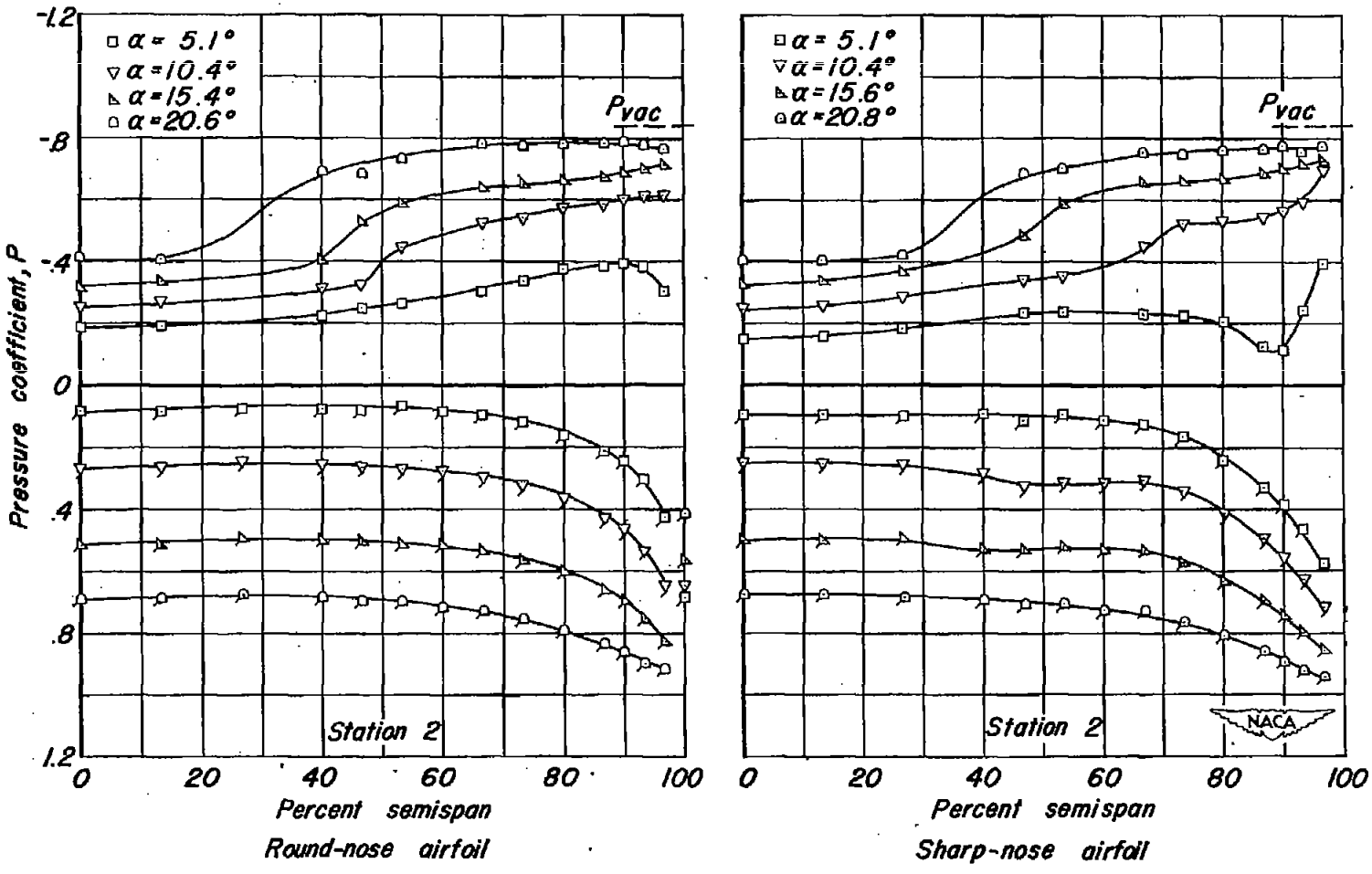

Figure 4.– Variation of pressure coefficient with angle of attack at Mach number 1.30. Flagged symbols denote lower surface.

(a) Round-nose airfoil.

(b) Sharp-nose airfoil.

Figure 5.- Effect of leading-edge profile on the flow characteristics of two-dimensional airfoils at $M = 0.80$. $\alpha = 4.0^{\circ}$.

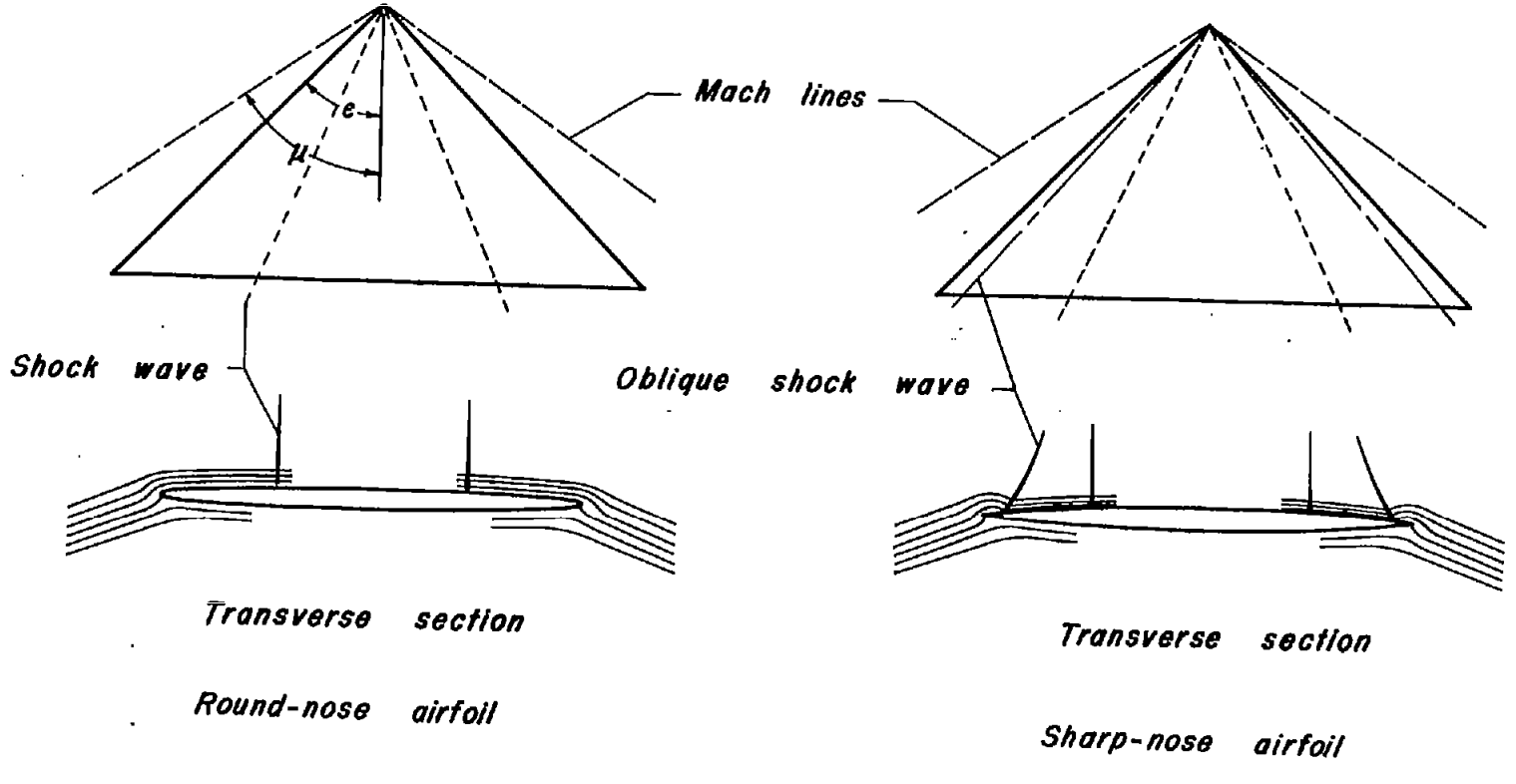

Figure 6.– Sketch of transonic flow phenomena for triangular wings swept behind the Mach lines.

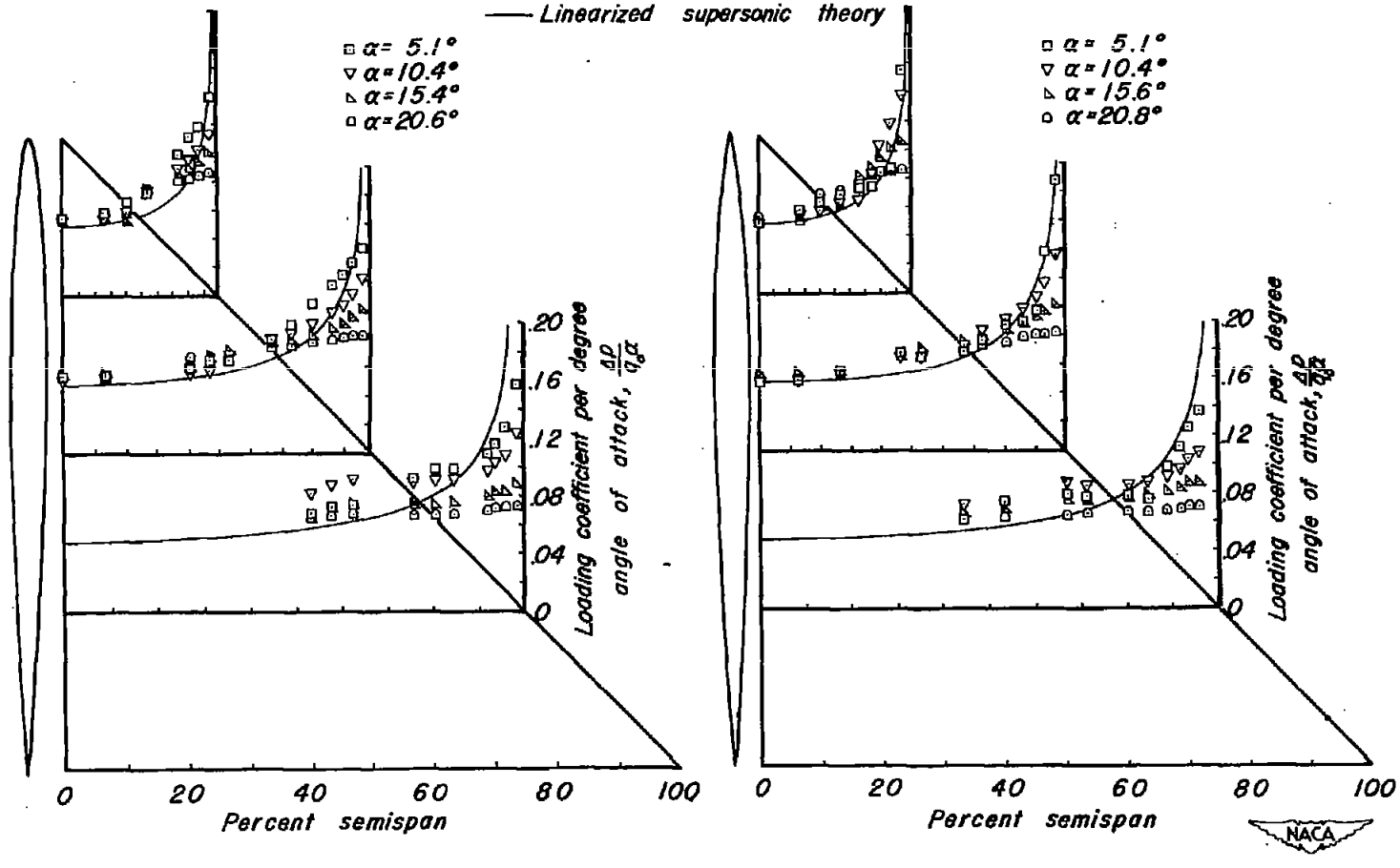

Figure 7.- Load distribution over triangular wings at Mach number 1.30.

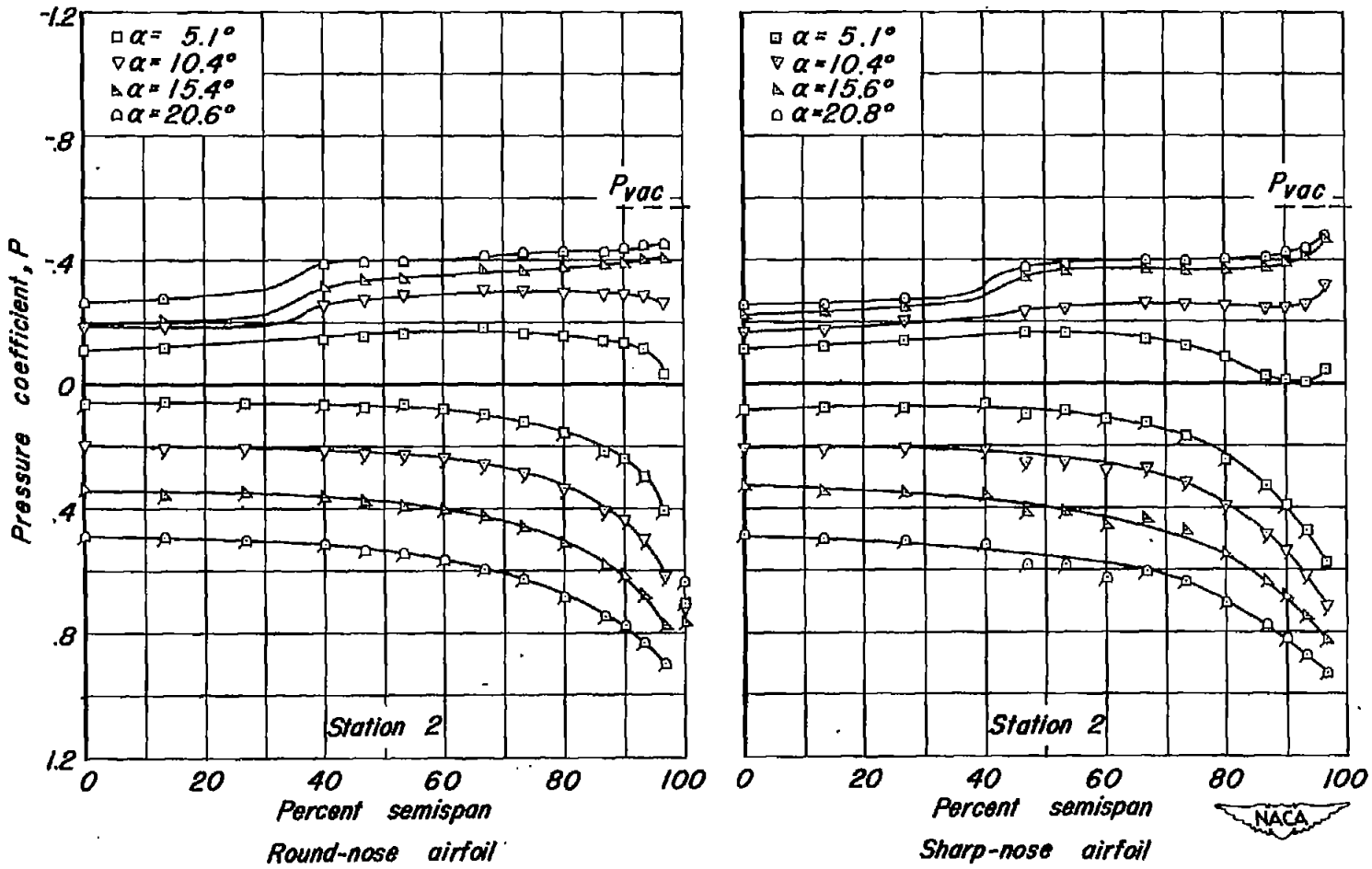

Figure 8.- Variation of pressure coefficient with angle of attack at Mach number 1.70. Flagged symbols denote lower surface.

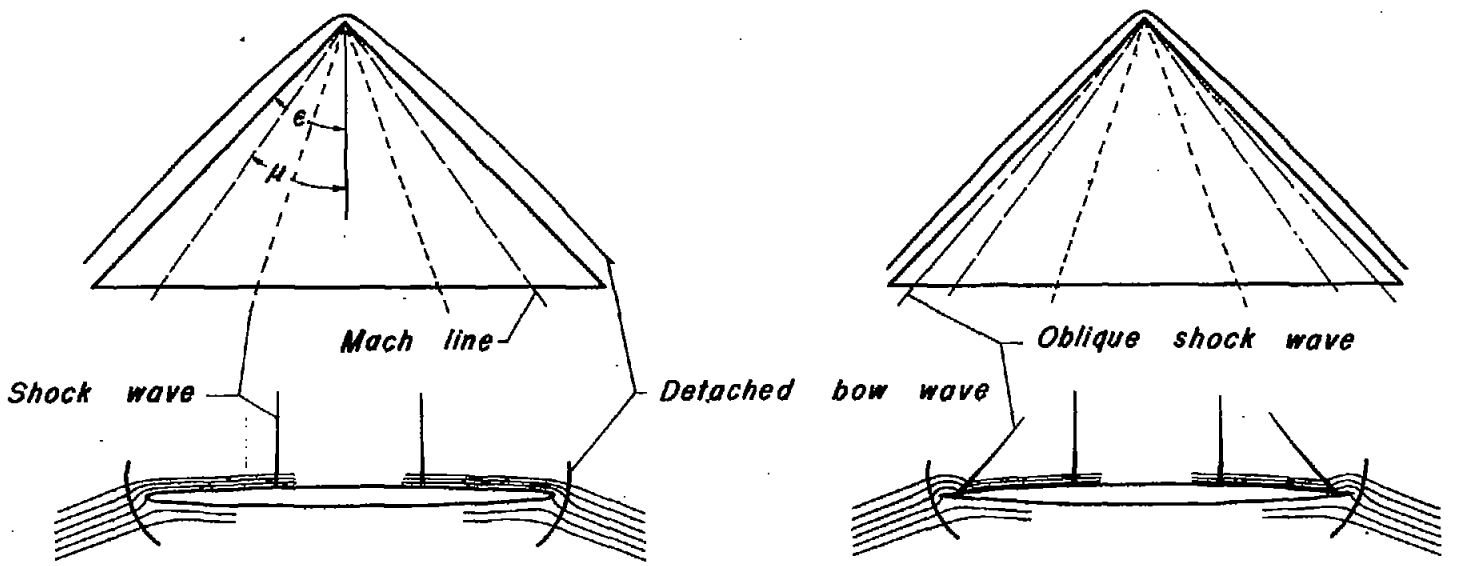

Figure 9.- Sketch of transonic flow phenomena for triangular wings swept ahead of the Mach lines.

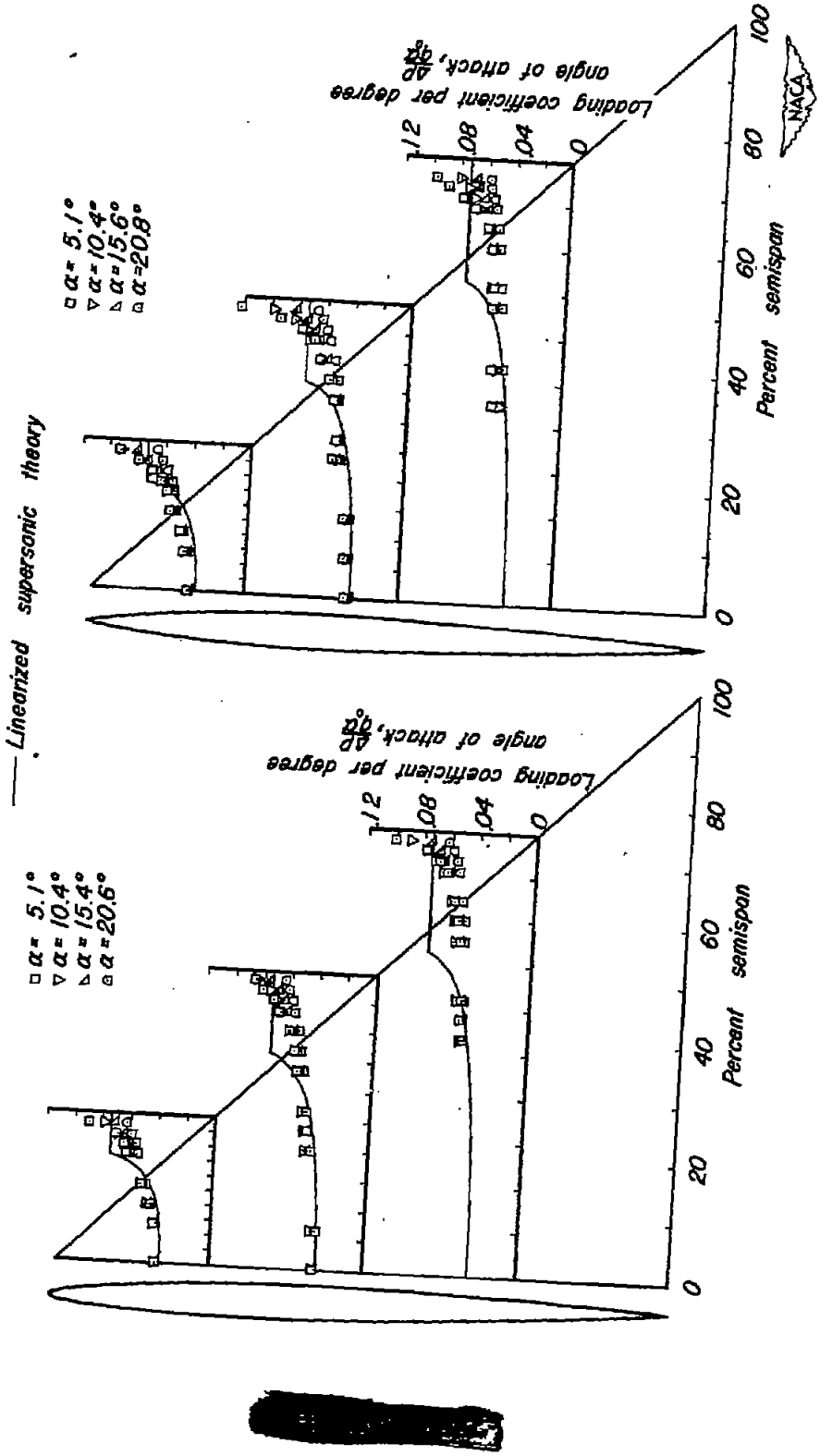

Figure 10.- Load distribution over triangular wings at Mach number 1.70.

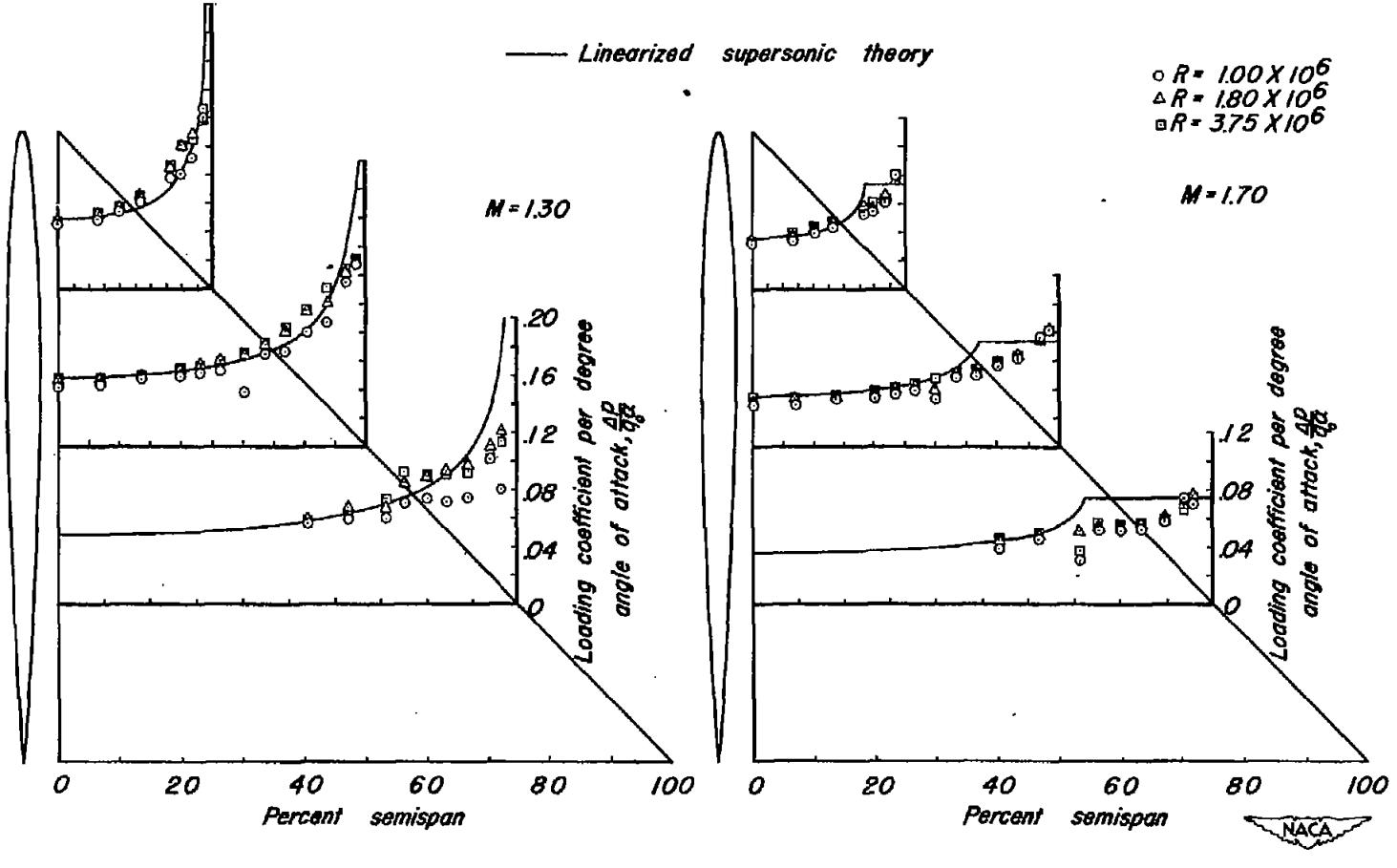

Figure 11.- Effect of Reynolds number on the load distribution over a triangular wing at $\alpha = 5.2°$.

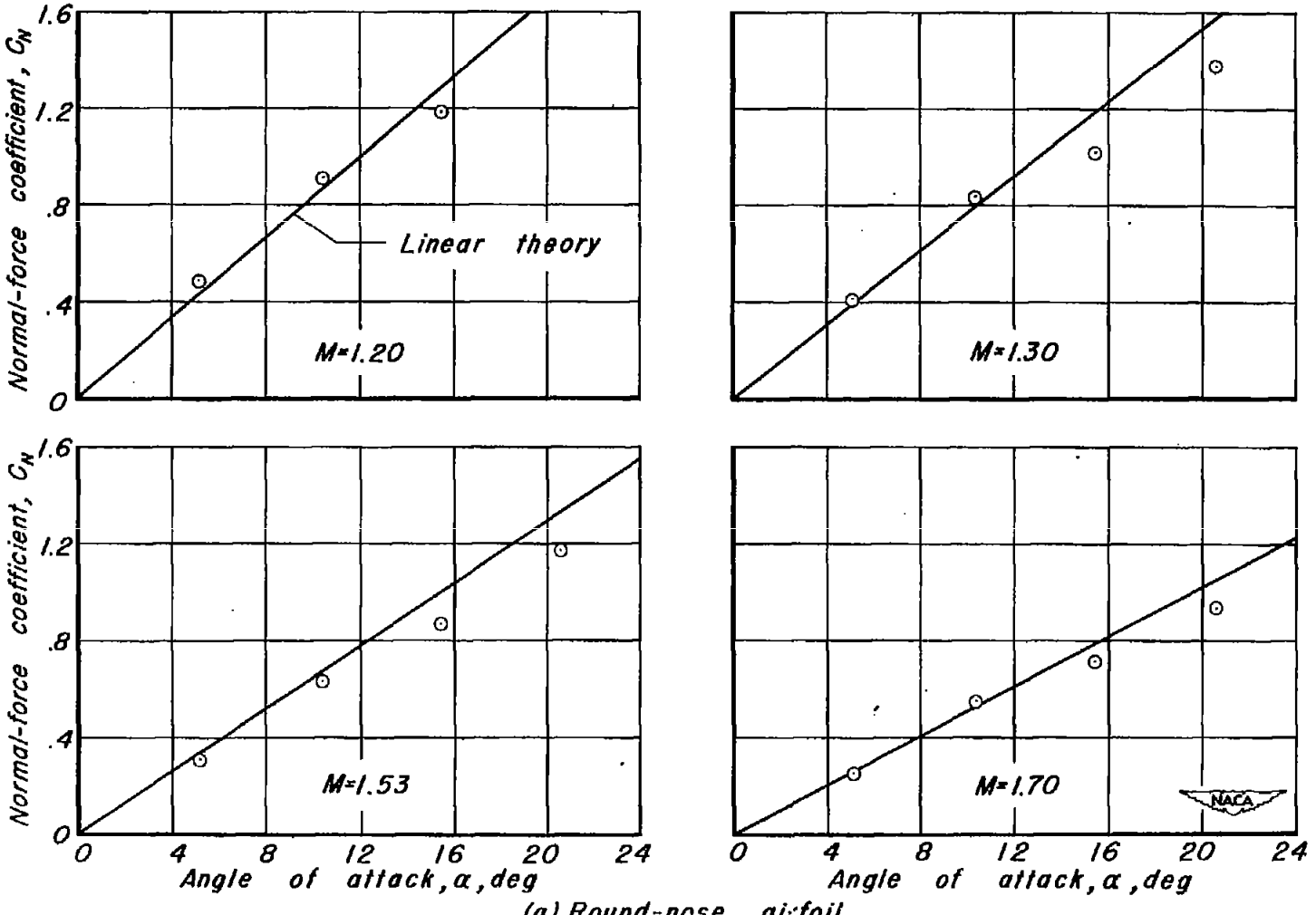

(a) Round-nose airfoil.

Figure 12.- Variation of the normal-force coefficient with angle of attack for several Mach numbers.

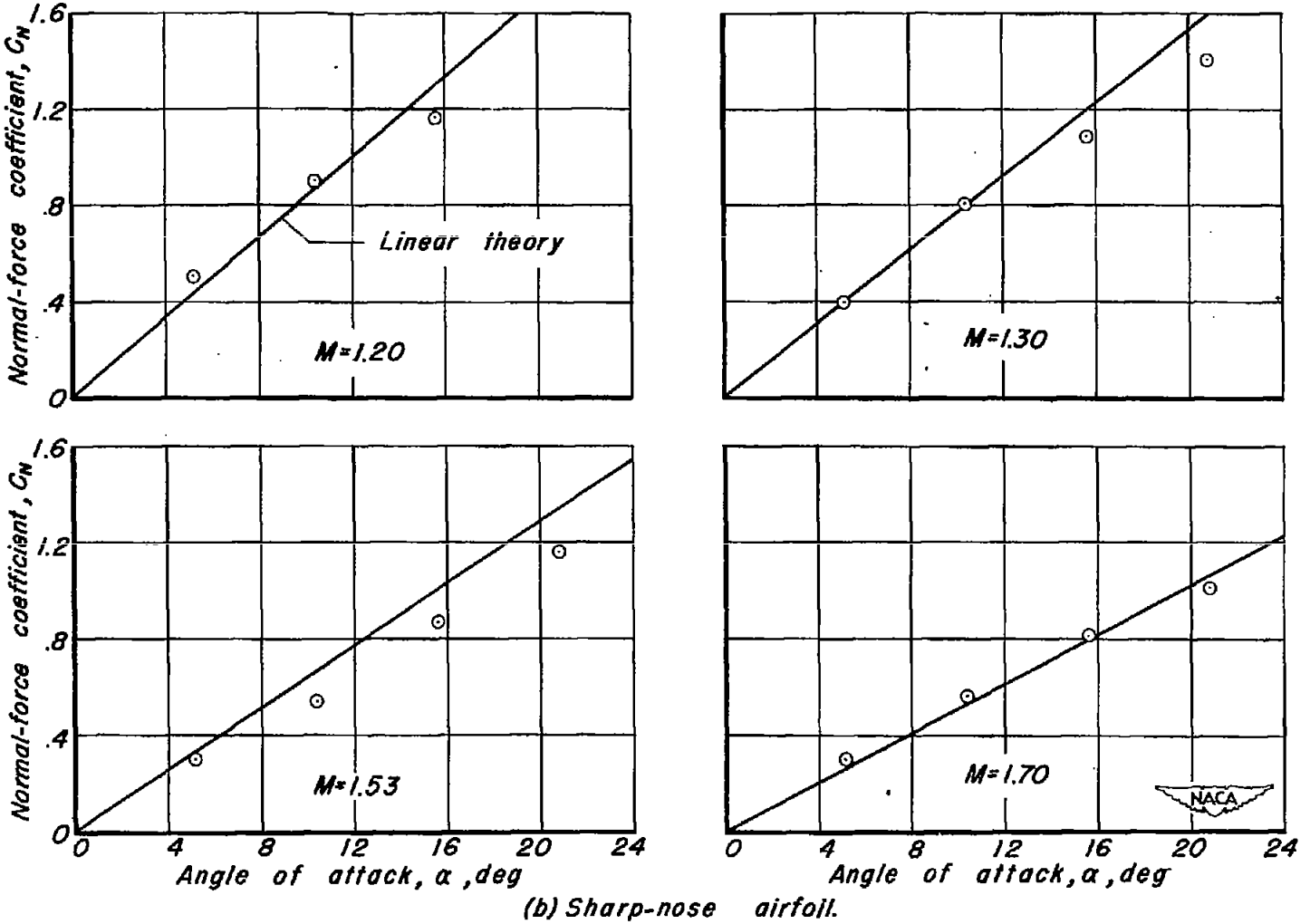

(b) Sharp-nose airfoil.

Figure 12.- Concluded.